P. Garbaczewski and R. Olkiewicz, Eds.,
Dynamics of Dissipation, Lectures Notes in Physics **597**
(Springer-Verlag, Berlin, 2002) pp. 111-164.

DYNAMICAL THEORY OF RELAXATION IN CLASSICAL AND QUANTUM SYSTEMS

Pierre Gaspard
Center for Nonlinear Phenomena and Complex Systems,
Faculté des Sciences, Université Libre de Bruxelles,
Campus Plaine, Code Postal 231, B-1050 Brussels, Belgium

An overview is given of recent work on the dynamical foundations of relaxation toward the thermodynamic equilibrium. The hydrodynamic modes play a central role in the relaxation. Recent advances show that exponentially decaying modes can be explicitly constructed at the microscopic level of description thanks to the concept of Pollicott-Ruelle resonance if the dynamics is hyperbolic. This construction is developed in detail for the irreversible processes of diffusion in the Lorentz gases and the multibaker models. These diffusion models are shown to obey the second law of thermodynamics according to which entropy production corresponds to the dissipation of energy.

I. INTRODUCTION

The advances in our knowledge of classical and quantum dynamics shed new lights on our understanding of the time evolution of the systems of interacting particles which compose matter. In particular, the discovery of chaotic dynamical systems has shown that a random time evolution is not incompatible with a deterministic law as given by Newton's equations. This remarkable result has suggested that many random processes in Nature may be governed by an underlying deterministic dynamics if this latter is chaotic.

In this perspective, the chaotic hypothesis appears as a principle of order. Indeed, a chaotic system naturally develops a milder dynamical randomness than the stochastic systems commonly used to model random processes. If the stochastic models are valid on relatively large spatial and temporal scales their validity becomes questionable on smaller scales where the deterministic dynamical rule manifests itself. In this regard, the chaotic hypothesis brings a missing link between the dynamic and the stochastic descriptions. Mathematical tools have been developed in order to characterize the dynamical randomness as well as the dynamical instability such as the Kolmogorov-Sinai (KS) and the ε-entropies per unit time and the Lyapunov exponents [1–3]. These characteristic quantities of chaos allow us to classify the different models of time evolution, in particular, in statistical mechanics [4].

Furthermore, the long-time relaxation to an asymptotic invariant statistical state can nowadays be characterized at the microscopic level of description in many systems of relevance to statistical mechanics. The long-time relaxation can already be characterized by the concept of mixing, which distinguishes between nondecaying and decaying time correlation functions, albeit ergodicity questions the unicity of the asymptotic invariant state [5]. The mixing property guarantees the statistical independency between two events separated by a long-time interval.[105] This statistical decorrelation turns out to play a fundamental role in nonequilibrium statistical mechanics because the transport coefficients are directly given in terms of the time correlation functions of the microscopic currents according to the Green-Kubo formulas [6, 7].

Moreover, the new concept of Pollicott-Ruelle resonance allows us to define at the microscopic level the exponential decay of statistical ensembles in systems of hyperbolic type [8–14] as well as in nonhyperbolic systems [15, 16]. It is at this place that a close connection appears with the macroscopic theory of transport and other irreversible processes where exponential decay are very common. Indeed, thanks to the Pollicott-Ruelle resonances, the exponential relaxation to the thermodynamic equilibrium can today be explained in great detail at the microscopic level of description in the phase space of spatially extended systems sustaining irreversible transport and reactive processes at their macroscopic level. In these systems, the relaxation to the thermodynamic equilibrium corresponds to the dissipation of work.

Besides, the Pollicott-Ruelle resonances also appear in the escape-rate theory of transport [17–19]. In this theory, the system is set out of equilibrium by absorbing boundary conditions. Accordingly, trajectories escape out of the system and the decay is characterized by an escape rate which is the leading Pollicott-Ruelle resonance of the system. The escape rate turns out to be given in terms of the positive Lyapunov exponents and the KS entropy, which establishes a relationship between transport and chaotic properties.

The Pollicott-Ruelle resonances have also been shown to be of importance to understand the relaxation in wave

and quantum systems [20–25]. In this context, a new regime of semiclassical relaxation, referred to in some papers as the "Lyapunov decay regime", has been identified beside the previously known deep quantum "golden rule decay regime" [26–28].

The purpose of these notes is to explain in detail the physical and mathematical bases of the connections between the macroscopic irreversible properties of relaxation and the underlying laws of time evolution of the microscopic dynamics and their characteristic features. These notes are organized in two different parts. A first part composed of Secs. II to IV deals with the classical systems, in the context of which the characteristic quantities of chaos as well as the Pollicott-Ruelle resonances have been developed. Section II describes the macroscopic phenomenology of the approach to the thermodynamic equilibrium with the hydrodynamic modes. Section III summarizes the tools of dynamical systems theory which are important to analyze and characterize the microscopic dynamics. The microscopic construction of the hydrodynamic modes and nonequilibrium steady states is overviewed in Sec. IV. The connection to thermodynamics is explained in Subsec. IV F for the processes of diffusion in the Lorentz gases, in which relaxation by diffusion is shown to correspond to the dissipation of work. A second part composed of Sec. V is concerned by the possible extension of these considerations to the understanding of relaxation in quantum systems.

II. MACROSCOPIC DESCRIPTION: THE HYDRODYNAMIC MODES

Let us start from the phenomenological description of macroscopic systems in order to explain how the concept of hydrodynamic mode is central to our understanding of the approach to the thermodynamic equilibrium.

The time evolution of macroscopic systems is described by the continuous-media partial differential equations such as the heat and diffusion equations, the Navier-Stokes equations, as well as the reaction-rate equations in chemical kinetics. The macroscopic equations are established starting from the laws of local conservation of mass, energy, linear momentum, and also angular momentum. Closed equations for the mean local variables are obtained by using phenomenological relations: firstly, for the equilibrium equations of states and, secondly, for the nonequilibrium relations between the currents and the gradients (or thermodynamic forces). The former phenomenological relations obey the laws of equilibrium thermodynamics while the latters obey those of irreversible thermodynamics and, especially, the second law of thermodynamics which requires the transport and reaction-rate coefficients of proportionality between the currents and the thermodynamic forces to be positive [29, 30].

The so-established macroscopic equations describe the large-scale properties of systems such as fluids, solids, reactive media, plasmas, etc... under equilibrium or nonequilibrium constraints. The constraints are imposed on the boundaries of the system and they determine whether the system will evolve to the state of thermodynamic equilibrium or not. An example of a system under equilibrium constraints is a glass of water which has been initially stirred. In this example, the fluid is transiently out of equilibrium but will eventually reach a state of macroscopic rest since the velocity field vanishes after a long enough time by the effect of viscosity. The description of this approach to the equilibrium is macroscopically described by linearizing the Navier-Stokes equations. The linearized Navier-Stokes equations must be solved by using the boundary conditions that the velocity field vanishes at the interface between the fluid and the glass. These boundary conditions select different modes of exponential decay known as the hydrodynamic modes. It is a very general result that the macroscopic equations predict such an approach to the equilibrium rest state by a linear combination of exponentially decaying modes.

This property also holds for spatially periodic modes in translationally invariant macroscopic systems. These spatially periodic modes are characterized by a wavelength λ or, equivalently, by a vector $\vec{k}$ of wavenumber $k = 2\pi/\lambda$ giving the wavelength in terms of its magnitude and the direction of the spatial periodic modulation by its orientation $\vec{k}/k$. These modes are the solutions of the linearized macroscopic equations behaving as

$$\exp\left(s_{\vec{k}}\, t + \mathrm{i}\, \vec{k}\cdot\vec{r}\right) \tag{1}$$

and they can be considered as the Fourier modes introduced by the spatial Fourier transform of the local variables describing the system. The time evolution of each mode is determined by the so-called *dispersion relation*

$$s_{\vec{k}} = \mathrm{Re}\; s_{\vec{k}} + \mathrm{i}\; \mathrm{Im}\; s_{\vec{k}} \tag{2}$$

The real part of $s_{\vec{k}}$ gives the decay rate of the modes and $\mathrm{Re}\, s_{\vec{k}} \leq 0$ because the system is expected to reach equilibrium for $t \to +\infty$. The imaginary part of $s_{\vec{k}}$ gives the frequency of oscillation of the modes. This frequency is nonvanishing for the propagative modes such as the sound modes but vanishes for the purely dissipative modes such as the thermal and diffusive modes.

It should be emphasized that the existence of spatially periodic and exponentially decaying solutions of the macroscopic equations does not mean that all the solution are exponentially decaying. Indeed, it is well-known that linear

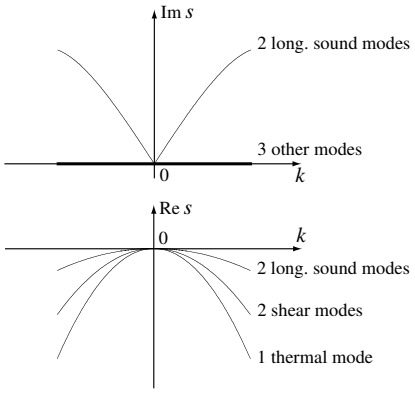

FIG. 1: Schematic dispersion relations of the five hydrodynamic modes of a normal fluid.

combinations of slower and slower exponential decays can lead to power-law decay. An example is given by the diffusion equation for which the dispersion relation is given by $s_{\vec{k}} = -\mathcal{D}k^2$. In this case, the integration of the Fourier modes (1) over vanishing wavenumbers $\vec{k}$ leads to the power-law decay $t^{-d/2}$ for $t \to \infty$, where d is the spatial dimension.

The modes can be distinguished by their behavior at large wavelength. The modes for which the rate $s_{\vec{k}}$ vanishes as the wavelength becomes infinite, $\lim_{\vec{k}\to 0} s_{\vec{k}} = 0$, are called the *hydrodynamic modes*. This is the case for the modes associated with the conserved quantities such as mass, energy, and momentum. Each globally conserved quantity is defined as the integral over the whole system of some combination of the local variables describing the system. Accordingly, the conserved quantity is given in terms of the spatial Fourier modes at zero wavenumber. Whereupon the time evolution of the modes associated with the conserved quantities must be frozen in the infinite wavelength limit so that $s_{\vec{k}=0} = 0$ for these modes.

An example of macroscopic systems illustrating this situation is a normal fluid composed of spherical particles carrying no angular momentum.[106] The five locally conserved quantities which are mass, energy, and the three components of linear momentum give five corresponding hydrodynamic modes [32–35]

- Two longitudinal sound modes which are propagative;
- Two shear modes which are purely dissipative;
- One thermal mode which is purely dissipative.

Their dispersion relation is schematically depicted in Fig. 1.

It should be noticed that kinetic modes may exist beside the hydrodynamic modes. The kinetic modes have the property that their damping rate does not vanish for $\vec{k} = 0$ so that they cannot be associated with conserved quantities. Usually, the kinetic modes are not easily identified at the macroscopic level of description but at the kinetic level by using for instance the Boltzmann equation in the case of dilute gases. The spectrum of kinetic modes depends on the interaction between the particles (as well as on the internal dynamics of the colliding particles such as rotation and vibration in the case of molecules). For a gas of spherical particles without internal structure, the kinetic modes have typically a damping rate of the order of the collision frequency. It is important to notice that the dynamics of relaxation to a local Maxwell-Boltzmann velocity distribution is controlled by the kinetic modes. Instead, the hydrodynamic modes rule the long-time evolution of the local macroscopic variables which are the mean local fluid velocity, density and temperature, the velocity distribution having locally reached its equilibrium Maxwell-Boltzmann distribution after a few intercollisional times. In the case of dilute gases, the spectrum of hydrodynamic and kinetic modes is obtained by linearizing the Boltzmann equation and finding the eigenvalues of the collision operator [31, 34, 36]. At very short wavelength of the order of the distance between the particles in dense fluids, the propagative hydrodynamic modes may present propagation gaps where the oscillation frequency vanishes, $\mathrm{Im}\, s_{\vec{k}} = 0$, as shown in Fig. 2 [37].

In systems with a mixture of several species of particles further hydrodynamic modes exist which correspond to the local conservation of the different species. If the fluid is composed of n species there are $(n-1)$ such modes of mutual diffusion [38].

If the different species undergo chemical reactions they are no longer conserved so that some of the hydrodynamic modes become kinetic modes with a nonvanishing decay rate at zero wavenumber. To illustrate this situation, we may consider the reaction of isomerization, $A \leftrightarrow B$, between two species A and B. The particles A and B are supposed to

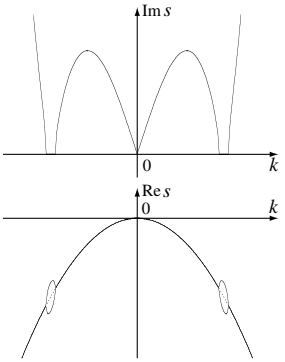

FIG. 2: Example of propagation gap in the dispersion relation of a sound mode.

diffuse in a solvent of inert particles, the whole fluid is at rest. This system is a ternary mixture in which we expect the five standard hydrodynamic modes plus two modes of mutual diffusion in absence of reaction. If the fluid is at rest and the reaction isothermal, the system can be modeled by two coupled diffusion-reaction equations [39–42]

$$\partial_t \rho_A = \mathcal{D}_{AA}\nabla^2\rho_A + \mathcal{D}_{AB}\nabla^2\rho_B - \kappa_+\rho_A + \kappa_-\rho_B \tag{3}$$

$$\partial_t \rho_B = \mathcal{D}_{BA}\nabla^2\rho_A + \mathcal{D}_{BB}\nabla^2\rho_B + \kappa_+\rho_A - \kappa_-\rho_B \tag{4}$$

Supposing solutions of the form (1) for Eqs. (3)-(4), we obtain two modes: a diffusive mode and a reactive mode. The diffusive mode has the dispersion relation:

$$s_{\vec{k}} = -\mathcal{D}\, k^2 + O(k^4) \tag{5}$$

with the diffusion coefficient

$$\mathcal{D} = \frac{\kappa_+(\mathcal{D}_{BB} + \mathcal{D}_{AB}) + \kappa_-(\mathcal{D}_{AA} + \mathcal{D}_{BA})}{\kappa_+ + \kappa_-} \tag{6}$$

The decay rate of this mode vanishes at $\vec{k} = 0$ so that it corresponds to the hydrodynamic mode of conservation of total mass of species A and B. The reactive mode has the dispersion relation:

$$s_{\vec{k}} = -\kappa_+ - \kappa_- - \mathcal{D}^{(\mathrm{r})}\, k^2 + O(k^4) \tag{7}$$

with the reaction rate $-s_0 = \kappa_+ + \kappa_-$ and the reactive diffusion coefficient

$$\mathcal{D}^{(\mathrm{r})} = \frac{\kappa_+(\mathcal{D}_{AA} - \mathcal{D}_{AB}) + \kappa_-(\mathcal{D}_{BB} - \mathcal{D}_{BA})}{\kappa_+ + \kappa_-} \tag{8}$$

Both dispersion relations are depicted in Fig. 3. We notice that the reactive mode becomes diffusive again if the reaction rates vanish, $\kappa_+ = \kappa_- = 0$, in which case the ternary mixture has two diffusive modes beside its five standard hydrodynamic modes, as expected. Accordingly, we conclude that some hydrodynamic diffusive modes turn into kinetic modes with $s_0 \neq 0$ in reacting systems. Very often these reactive modes are observed at the macroscopic level because their decay rates are of the order of the inverse of reaction rates in the range of seconds, minutes, or more. This is the case for the typical reactions studied in chemical kinetics at the beginning of the XXth century [43]. In the second half of the XXth century, faster and faster chemical reactions have been studied bringing the inverse reaction rates down to the time scale of the picoseconds and below [44]. Such ultrafast reactions evolve on the picosecond time scale of the kinetic modes of inert fluids and even on faster time scales. It is therefore appropriate to consider the reactive modes as some kind of kinetic modes.

Hydrodynamic modes, i.e., modes with a vanishing dispersion relation at infinite wavelength, also arises in systems undergoing the spontaneous breaking of a continuous symmetry. These hydrodynamic modes are often referred to as Goldstone modes [45]. For instance, a breaking of continuous symmetry occurs in the fluid-solid transition at which the system looses its continuous translational symmetry in the three spatial directions. Accordingly, solids have three extra hydrodynamic modes beside those associated with the five fundamental conserved quantities which are the three components of linear momentum, energy, and mass. Solids have therefore eight hydrodynamic modes which are known to be [46]

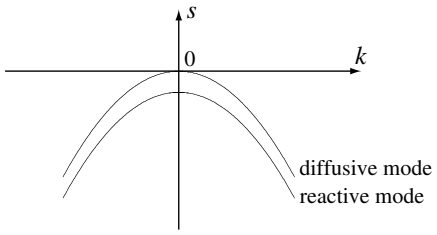

FIG. 3: Schematic dispersion relations of the diffusive and reactive modes of a reaction of isomerization $A \leftrightarrow B$ taking place in a fluid solvent at rest.

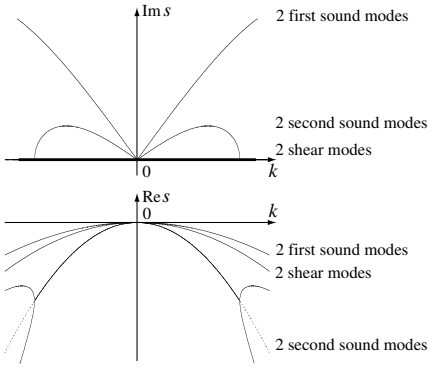

FIG. 4: Schematic dispersion relations of the six hydrodynamic modes of a superfluid.

- Two longitudinal sound modes which are propagative;
- Four transverse sound modes which are propagative;
- One thermal mode which is purely dissipative;
- One mode of vacancy diffusion which is purely dissipative.

Another example of continuous symmetry breaking occurs in the fluid-superfluid transition. In the superfluid phase, the superfluid coexists with the normal fluid and is characterized by an order parameter which breaks a continuous gauge symmetry. Since the order parameter is a scalar one Goldstone modes adds to the five hydrodynamic modes of a normal fluid, leading to a total of the six following hydrodynamic modes [47]

- Two first sound modes which are propagative;
- Two second sound modes which are propagative;
- Two shear modes which are purely dissipative.

Their dispersion relation is schematically depicted in Fig. 4.

These different examples show the fundamental importance of the hydrodynamic modes for the understanding of the time evolution of different materials and, especially, the approach to the equilibrium rest state in each system. The existence of these hydrodynamic modes emphasize the importance of the exponential decay to the thermodynamic equilibrium. The exponential decay is one of the most compeling expression of the irreversibility of the approach to the thermodynamic equilibrium. We may wonder how such exponential decay are compatible with the underlying microscopic dynamics which is known to be Hamiltonian and time-reversal symmetric. This question brings us to the study of the microscopic dynamics.

III. GENERALITIES ABOUT THE MICROSCOPIC DYNAMICS

All the systems of Nature are observed to be of Hamiltonian type at their microscopic level. It turns out that the observation of nonHamiltonian behavior has always been found to have its origin in the existence of previously ignored

degrees of freedom and a Hamiltonian description has always been recovered by including the neglected degrees of freedom. We should probably understand the importance of the Hamiltonian framework as due to the fact that time translations are naturally generated by the energy operator in quantum mechanics.

The Hamiltonian of electromagnetic interaction, which rules the low-energy macroscopic world, is known to be time-reversal symmetric whereupon the motion of atoms and molecules is assumed to be ruled by a time-reversal symmetric Hamiltonian. Fluids are very well described by the Hamiltonian of atoms or molecules interacting through the van der Waals interactions[107]

$$H = \sum_{i=1}^{N} \frac{\vec{p}_i^{\,2}}{2m} + \frac{1}{2} \sum_{i \neq j} V(\|\vec{r}_i - \vec{r}_j\|) \tag{9}$$

where $V(r)$ is the interaction potential. This system has $f = Nd$ degrees of freedom if the physical space has dimension d. The time evolution is time-reversal symmetric because

$$H\left(\{\vec{r}_i, -\vec{p}_i\}\right) = H\left(\{\vec{r}_i, \vec{p}_i\}\right) \tag{10}$$

At room temperature, the de Broglie wavelength of the particles is much shorter than their mean free path so that classical mechanics provides an excellent description according to Hamilton's equations:

$$\begin{cases} \dot{\vec{r}}_i = +\dfrac{\partial H}{\partial \vec{p}_i} \\ \dot{\vec{p}}_i = -\dfrac{\partial H}{\partial \vec{r}_i} \end{cases} \tag{11}$$

with $i = 1, 2, ..., N$.

We notice that the Hamiltonian assumption is stronger than the fulfilment of the conservation of energy since it imposes a symplectic structure to the microscopic time evolution. One of the consequences of this symplectic structure is Liouville's theorem that volumes $d^f r d^f p$ are preserved in phase space [48].

The time integration of Hamilton's equations uniquely determines the trajectories $\Gamma_t = \{\vec{r}_i(t), \vec{p}_i(t)\}$ in terms of their initial conditions $\Gamma_0 = \{\vec{r}_i(0), \vec{p}_i(0)\}$. We denote by $\Gamma_t = \Phi^t \Gamma_0$ the *flow* induced in phase space by Hamilton's equations.

A. The Poincaré map

A very powerful tool in the analysis of continuous-time dynamical systems is provided by the *Poincaré map* [3, 30]. The idea is to intersect the trajectories of the flow Φ^t by a surface of section introduced in phase space. Each trajectory will thus generate a sequence of intersection points $\{\Gamma_n\}$. Since the system is deterministic the knowledge of an intersection point determines the next one. Accordingly, the flow induces the Poincaré map:

$$\begin{cases} \Gamma_{n+1} = \Phi^{T(\Gamma_n)}(\Gamma_n) \equiv \phi(\Gamma_n) \\ t_{n+1} = t_n + T(\Gamma_n) \end{cases} \tag{12}$$

where $\{t_n\}$ denote the intersection times which are controled by the first-return time function $T(\Gamma)$ [3]. The Poincaré map provides a description of the system which is strictly equivalent to the flow, given that each segment of trajectory between two successive intersections can be reconstructed.

An example of Poincaré map is the Birkhoff map in billiards where the trajectory moves in free flight between the collisions [3]. The Birkhoff map is the mapping from each collision to the next. In two-dimensional billiards, each collision can be represented by the so-called Birkhoff coordinates: the arc of perimeter $r_\parallel$ of the impact point and the momentum $p_\parallel$ tangent to the border of the billiard at the impact. The free flight from one collision to the next induces a mapping of Birkhoff's coordinates, $(r_{\parallel,n+1}, p_{\parallel,n+1}) = \phi(r_{\parallel,n}, p_{\parallel,n})$, which is known to be area preserving. In this way, the continuous-time dynamics of a billiard such as the two-dimensional Lorentz gas can be described by an area-preserving mapping, which can greatly simplify the analysis while keeping the strict equivalence with the continuous-time dynamics [3].

B. Statistical ensembles and their time evolution

The Newtonian scheme does not fix the initial conditions to be used for Newton's equations. In many experiments, the initial conditions are fixed by the preparation of the system under study. For instance, in artillery, the initial

condition of the cannon-ball is determined by the cannon, which is a mechanical device *external* to the system determining the parabolic trajectory of the cannon-ball. It is in general impossible to achieve the perfect reproducibility of the initial condition from one experiment to the next. Therefore, the initial conditions are always submitted to some uncertainty, which can be modeled by repeating many times the experiment and establishing the statistics of the initial conditions. The statistical description defines the probability density of initial conditions as

$$f_0(\Gamma) = \lim_{M\to\infty} \frac{1}{M} \sum_{m=1}^{M} \delta(\Gamma - \Gamma_0^{(m)}) \tag{13}$$

where M is the number of performed experiments with the idea that this number should be large enough in order for the initial density $f_0(\Gamma)$ to be represented by a smooth function of Γ.

In laboratory experiments on matter, the initial conditions are also submitted to uncertainty. Often, the experiment starts at a given initial time when the system is in a state of stationarity for as many quantities as can possibly be monitored by measuring devices. Since the resolution of the measuring devices is always finite the initial conditions are not reproducible and will vary from one experiment to the next. This nonreproducibility requires the use of statistical considerations and the description of the initial conditions by a probability density such as (13).

From the initial condition, the system is supposed to be left to itself so that the trajectory evolves according to Hamilton's equations in each repetition of the experiment. Because of the sensitivity to initial conditions which is the feature of chaotic systems, the prediction of the time evolution of the individual trajectories is vain beyond the time of divergence of trajectories from nearby initial conditions [30]. Instead, predictions remain fruitful for statistical quantities such as averages or correlation functions which are described in terms of the probability density of the trajectories defined as

$$f_t(\Gamma) = \lim_{M\to\infty} \frac{1}{M} \sum_{m=1}^{M} \delta(\Gamma - \Gamma_t^{(m)}) \tag{14}$$

The time evolution of this probability density is induced by Hamilton's equations and is known to be ruled by the Liouville equation

$$\partial_t f = \hat{L} f \equiv -\mathrm{div}\left(\dot{\vec{\Gamma}} f\right) = \{H, f\} \tag{15}$$

where $\{\cdot,\cdot\}$ denotes the Poisson bracket of classical mechanics. The time integral of Liouville's equation defines the Frobenius-Perron operator which is given by

$$f_t(\Gamma) = \hat{P}^t f_0(\Gamma) = \mathrm{e}^{\hat{L}t} f_0(\Gamma) = f_0(\Phi^{-t}\Gamma) \tag{16}$$

for time-independent systems. The last equality is a consequence of Liouville's theorem. The probability density can then be used to calculate the statistical averages of the physical observables:

$$\langle A\rangle_t \;=\; \int A(\Gamma)\; f_t(\Gamma)\; d\Gamma = \langle A|\hat{P}^t|f_0\rangle \tag{17}$$

Very often, the system under study is not isolated but in contact with other systems through walls. This is the case for a fluid in a container. After a time interval, the bulk of the fluid becomes determined by the state of the walls of the container and, in particular, by their temperature. At the wall, the atoms of the fluid interact with the atoms of the wall via short-ranged interactions. The description of this interaction implies to suppose that the whole system composed of the fluid plus its surrounding is Hamiltonian. If the description is reduced to the sole degrees of freedom of the fluid, the equations of motion typically become Langevin stochatic differential equations of the form of Hamilton's equations plus extra forces describing the stochastic forcing of the fluid degrees of freedom by the surrounding and the associated dissipation from the fluid to the surrounding [49].

If the temperature of the surrounding is uniform and if the system does not sustain a net flux of matter, the system is expected to reach a state of thermodynamic equilibrium for typical statistical ensembles of initial conditions. This is the case for the initially stirred glass of water described here above. The description of such an experiment of approach to the thermodynamic equilibrium is most often simplified by ignoring the stochastic forcing at the wall and supposing that the fluid particles undergo elastic collisions on the wall of the container. In this way, the boundary stochastic forcing is replaced by *reflecting boundary conditions* which require that the probability current ingoing the wall exactly compensate the outgoing current so that no particle remains stuck at the wall. For reflecting boundary conditions, the system is typically expected to evolve toward a microcanonical statistical state of thermodynamic

equilibrium at the total energy of the initial conditions. The convergence to the microcanonical state should be understood as a weak convergence holding only for statistical averages such as (17).

For the purpose of computing the viscosity or other quantities of interest by molecular dynamics, *periodic boundary conditions* are often used to simplify the dynamics. These boundary conditions are implemented by supposing that the system is composed of N particles moving on a torus obtained by identifying two-by-two the opposite boundaries of a cell tessellating the physical space. For periodic boundary conditions, the system is typically expected to evolve toward a microcanonical statistical state of thermodynamic equilibrium at the total energy and linear momentum of the initial conditions.

In many systems of interest, the surrounding is not in equilibrium, for instance, because different walls are at different temperatures or, more generally, because there is an exchange of matter under the form of a flux of particles from one reservoir to another. Typical experiments in which such fluxes are essential are the laminar or turbulent flows in pipes or around an object as studied in fluid mechanics, or flows of chemical species in a continuously stirred tank reactor as used in nonequilibrium chemical kinetics [30]. Another example is given by the study of diffusion of tracer particles through slabs of fluids or even solids sandwitched between two reservoirs [50]. In these different systems, a fictitious boundary delimits an open system through which matter is exchanged. The number of particles inside the system fluctuates so that the state of the system should be described by a sort of classical analog of the Fock space introduced in the study of many-body quantum systems. Indeed, the system may contain a varying number of particles and, for each number N of particles, the system is described by a probability density such as (14):

$$\mathbf{f} = \left\{ f^{(0)}, f^{(1)}(\vec{r}_1, \vec{p}_1), f^{(2)}(\vec{r}_1, \vec{p}_1, \vec{r}_2, \vec{p}_2), ..., f^{(N)}(\vec{r}_1, \vec{p}_1, ..., \vec{r}_N, \vec{p}_N), ... \right\} \tag{18}$$

The probability that the system contains N particles is given by

$$P_N = \int f^{(N)}(\vec{r}_1, \vec{p}_1, ..., \vec{r}_N, \vec{p}_N)\, d\vec{r}_1\, d\vec{p}_1\, \cdots\, d\vec{r}_N\, d\vec{p}_N \tag{19}$$

which is normalized by

$$\sum_{N=0}^{\infty} P_N = 1 \tag{20}$$

Under similar circumstances as the stochastic forces due to the surrounding can be modeled by reflecting or periodic boundary conditions at equilibrium, we can here also take into account of the nonequilibrium constraints from the surrounding by appropriate boundary conditions which fix the probability currents ingoing the system at its boundaries. The advantage of this description is that the Hamiltonian character of the time evolution is maintained in the whole description. A typical trajectory of the system is a sequence of segments of trajectories of Hamiltonian N-body systems, N being the number of particles in the system during each segment of trajectory. During each segment, all the particles are contained inside the boundaries delimiting the open system and the trajectory belongs to some phase space $\mathcal{M}^{(N)}$ which is limited in position.

Each probability density in Eq. (18) obeys a N-body Liouvillian equation:

$$\partial_t f^{(N)} = \hat{L}^{(N)} f^{(N)} = \{H^{(N)}, f^{(N)}\} \tag{21}$$

with appropriate boundary conditions. The probability that the system contains N particles evolves in time according to

$$\frac{dP_N}{dt} = \int_{\mathcal{M}^{(N)}} d\Gamma^{(N)} \{H^{(N)}, f^{(N)}\} \tag{22}$$

$$= -\int_{\mathcal{M}^{(N)}} d\Gamma^{(N)}\, \mathrm{div}\left(\dot{\vec{\Gamma}}^{(N)} f^{(N)}\right) \tag{23}$$

$$= -\int_{\partial\mathcal{M}^{(N)}} d\vec{\Sigma}^{(N)} \cdot \dot{\vec{\Gamma}}^{(N)}\, f^{(N)} \tag{24}$$

$$= \underbrace{-\int_{\partial\mathcal{M}^{(N)}_{\mathrm{in}}} d\vec{\Sigma}^{(N)} \cdot \dot{\vec{\Gamma}}^{(N)}\, f^{(N)}}_{\geq 0} \underbrace{-\int_{\partial\mathcal{M}^{(N)}_{\mathrm{out}}} d\vec{\Sigma}^{(N)} \cdot \dot{\vec{\Gamma}}^{(N)}\, f^{(N)}}_{\leq 0} \tag{25}$$

where the first term of the last equality is fixed by the boundary conditions.

These considerations provide a fairly general framework to describe a large variety of nonequilibrium systems while preserving the Hamiltonian and Liouvillian properties. Open systems exchanging matter with its surrounding can be described by imposing *flux boundary conditions* that the ingoing probability currents at the boundaries be fixed according to the concentrations and velocity distributions of the different species of ingoing particles. We notice that such a framework has already been developed for solving Boltzmann's equation in nonequilibrium systems. Such considerations are here generalized to Liouville's equation. Nonequilibrium systems between heat reservoirs at different temperatures can also be modeled with flux boundary conditions by supposing that the ingoing particles have a Maxwellian velocity distribution at the temperature of the heat reservoir. Since Liouville's theorem is strictly preserved in the present framework we could here speak about *Liouvillian thermostats*. Systems such as a fluid undergoing the Rayleigh-Bénard convection or nonlinear chemical reactions sustaining nonequilibrium oscillations can be described in this framework.

After a long time, the system is supposed to reach a stationary state which is a nonequilibrium steady state if the boundary conditions are of nonequilibrium type. In such a stationary state driven by *flux boundary conditions*, each probability (19) should reach a nonvanishing constant value so that the ingoing and outgoing fluxes of probability given by the two terms of the last line of Eq. (25) balance each other. Such a stationary state should in general be described by a vector of probability densities (18) which is very different from the equilibrium densities. At stationarity, this vector defines the invariant probability measure describing the statistical steady state of the system.

Among the different possible boundary conditions, the *absorbing boundary conditions* play a special role. These boundary conditions may be imposed on a system with a fixed number N of particles by supposing that there is no ingoing flux of probability (or particle). Therefore, the first term in the last line of Eq. (25) vanishes and the probability $P_N(t)$ monotonously decays to zero as time increases. Here, the interesting properties manifest themselves in the way the decay of $P_N(t)$ proceeds. If the decay is asymptotically exponential the decay rate defines the so-called *escape rate* used in the escape-rate theory of transport. Under certain circumstances, an invariant probability measure can still be defined in the presence of absorbing boundary conditions as explained in Subsection IV C.

C. Ergodicity and mixing

The construction of the invariant measure mentioned in the previous discussion is an important issue in order to understand the long-time approach of a system to a stationary statistical state.

In closed deterministic systems in which the number of particles is conserved, a natural invariant measure is selected by time averaging the quantities of interest over a given trajectory. Birkhoff's ergodic theorem, that

$$\lim_{T\to\infty} \frac{1}{T} \int_0^T A(\Phi^t \Gamma_0)\, dt = \int A(\Gamma)\, \mu(d\Gamma) \tag{26}$$

for μ-almost all initial conditions Γ_0 [5], provides a decomposition of the phase space into ergodic components which are the support of the different invariant measures μ constructed by the time average. A system is commonly said to be ergodic if its smallest ergodic components are the energy shells or the energy-momenta shells. The corresponding invariant measures μ define the statistical ensembles which can be identified with the thermodynamic equilibria.

In open systems with absorbing boundary conditions, a unique ergodic normalizable measure can be defined on the invariant set of trajectories which are forever trapped inside the system under the condition that this set is transitive, i.e., contains a dense trajectory. Otherwise, the invariant set should be decomposed into different ergodic components in a similar way as for closed systems. In open systems with flux boundary conditions, ergodic invariant measures can be defined by reference to the random process induced by the dynamics and the boundary conditions.

In closed or open systems, the relaxation toward a supposed unique invariant measure μ is guaranteed by the property of *mixing* which has been introduced by Gibbs [51] and which is defined by the condition that [5]

$$\lim_{t\to\infty} \mu(\Phi^{-t}\mathcal{A} \cap \mathcal{B}) = \mu(\mathcal{A})\, \mu(\mathcal{B}) \tag{27}$$

where $\mathcal{A}$ and $\mathcal{B}$ are two sets in phase space. The mixing property guarantees the statistical independency between the random events that the trajectory be in the set $\mathcal{B}$ at time $t = 0$ and in the set $\mathcal{A}$ at time t, in the long-time limit $t \to \infty$. The definition (27) implies that the time correlation functions defined by statistical average over the invariant measure μ decays to their stationary values as

$$\lim_{t\to\infty} \langle A(\Phi^t \Gamma)\, B(\Gamma)\rangle_\mu = \langle A\rangle_\mu\, \langle B\rangle_\mu \tag{28}$$

where $\langle X\rangle_\mu = \int X(\Gamma)\, \mu(d\Gamma)$.

D. Dynamical instability

Besides the mere knowledge of the trajectories it is often important to characterize their stability and, in particular, their linear stability which is the behavior of infinitesimal perturbations $\delta\Gamma_t = \{\delta\vec{r}_i(t), \delta\vec{p}_i(t)\}$ on each trajectory. These perturbations evolves in time under the linearized Hamiltonian equations:

$$\begin{cases} \delta\dot{\vec{r}}_i = +\sum_{j=1}^{N} \left(\frac{\partial^2 H}{\partial \vec{p}_i \partial \vec{r}_j} \cdot \delta\vec{r}_j + \frac{\partial^2 H}{\partial \vec{p}_i \partial \vec{p}_j} \cdot \delta\vec{p}_j \right) \\ \delta\dot{\vec{p}}_i = -\sum_{j=1}^{N} \left(\frac{\partial^2 H}{\partial \vec{r}_i \partial \vec{r}_j} \cdot \delta\vec{r}_j + \frac{\partial^2 H}{\partial \vec{r}_i \partial \vec{p}_j} \cdot \delta\vec{p}_j \right) \end{cases} \tag{29}$$

with $i = 1, 2, ..., N$. The infinitesimal perturbations may remain bounded or grow as a power of time, or even exponentially. The exponential growth is the fastest possible growth in a system described by ordinary differential equations. This form of dynamical instability is characterized by the so-called *Lyapunov exponents* [1]

$$\lambda = \lim_{t\to\infty} \frac{1}{t} \ln \frac{\|\delta\Gamma_t\|}{\|\delta\Gamma_0\|} \tag{30}$$

in closed systems with a constant number N of particles. We may have as many different Lyapunov exponents as there are different directions in phase space so that the total number of Lyapunov exponents is equal to the phase-space dimension $2f = 2Nd$. The Lyapunov exponents may vary from one trajectory to another.

The Hamiltonian character implies a pairing rule among the different Lyapunov exponents due to the symplectic property: To each Lyapunov exponent λ_i, there corresponds another one which is $-\lambda_i$ [3].

Several Lyapunov exponents vanish which are associated with the conserved quantities such as energy or linear momentum when they exist. The pairing rule implies that, to each vanishing Lyapunov exponent associated with a conserved quantity, there corresponds another vanishing Lyapunov exponent. In the case of the vanishing Lyapunov exponent associated with energy, the other vanishing Lyapunov exponent is the one associated with the direction of the flow.[108] In Hamiltonian systems, the number of vanishing Lyapunov exponents is thus always even by the symplectic property.

Systems with positive Lyapunov exponents are dynamically unstable. Typical Hamiltonian systems have dynamically unstable trajectories, in particular, by the formation of homoclinic orbits. However, typical Hamiltonian systems also present quasiperiodic trajectories with all their Lyapunov exponents vanishing. In Hamiltonian systems with two degrees of freedom, these quasiperiodic trajectories exist inside elliptic islands coexisting with zones filled with unstable trajectories. The quasiperiodic trajectories occupy the largest phase-space volume in systems close to integrability according to the KAM theorem, which is the case for systems such as Hamiltonian chains of coupled anharmonic oscillators at very low energy or temperature [52, 53]. However, at high energy or temperature, the quasiperiodic trajectories are numerically observed to shrink while the unstable trajectories fill the largest part of phase space. This phenomenon is observed, in particular, in the standard map where the elliptic islands become tiny and practically inobservable at large values of the parameter although they exist for a dense set of parameter values [54].

Systems are said to be *hyperbolic* if the positive Lyapunov exponents associated with the different directions and trajectories of the system remain separated from zero by a gap: $\lambda_i \geq \lambda_{\min} > 0$. However, typical Hamiltonian systems such as the standard map are nonhyperbolic because the quasiperiodic trajectories have vanishing Lyapunov exponents and, furthermore, trajectories close to the quasiperiodic ones may have arbitrarily small positive Lyapunov exponents.

The spectrum of Lyapunov exponents is best known for billiards with convex boundaries such as the Sinai billiard, the Lorentz gas, or the finite hard-sphere gases. In these systems, almost all the trajectories have positive Lyapunov exponents which are well separated from zero. However, there exist sets of zero Lebesgue measure of trajectories with all their Lyapunov exponents vanishing because these trajectories never bounce on a convex boundary. Under certain conditions, these special trajectories do not exist as in the periodic Lorentz gas on a triangular lattice with a finite horizon [3].

Beside the dynamically unstable billiards, we also find the polygonal billiards [55] such as the wind-tree model [56], in which the boundaries are flat so that all the Lyapunov exponents vanish. In polygonal billiards, infinitesimal perturbations grow as a power of time but never exponentially.

Beyond the closed systems, the open systems are of great importance in nonequilibrium conditions and, especially, in scattering experiments [3, 14, 20]. In scattering systems, the majority of trajectories are coming from and returning to infinity. These systems are typically out of equilibrium with a possible steady state fixed by the velocity distribution and the spatial profile of the beams of incoming particles. An example of scattering systems is given by a particle moving in a one-dimensional potential with a maximum above two valleys of asymptotically free motion. Other

examples are the disk scatterers. In these open systems, the trajectories which control the long-time escape are those which are trapped inside the system. The forever trapped trajectories are unstable with positive Lyapunov exponents and form an invariant set which is of zero Lebesgue measure. Open systems can be dynamically unstable without being chaotic. This is the case for the point particle on the maximum of a potential as well as for the particle periodically bouncing on the line joining the centers of two disks in the two-disk scatterer.

For the system to be chaotic, we need more than a positive Lyapunov exponent: we need a random time evolution, the characterization of which requires to introduce another quantity than the Lyapunov exponent.

E. Dynamical randomness

The definition of dynamical randomness requires the introduction of the so-called Kolmogorov-Sinai (KS) entropy per unit time [1, 5]. The KS entropy is defined as the supremum of the decay rates of the multiple time probabilities for the trajectory to successively visit different cells in phase space. Let us suppose that the phase space is partitioned into cells forming a partition $\mathcal{P}$. If ω_n denotes the label of the cell visited by the trajectory at time $t = n\Delta t$, the multiple time probabilities would decay exponentially if the motion of the system is random:

$$\mu(\omega_0\omega_1\cdots\omega_{n-1}) \sim \exp\left(-n\ \Delta t\ h_{\mathcal{P}}\right) \qquad \text{for } n \to \infty \tag{31}$$

The exponential decay here goes with the number n of visited cells and not with the time interval Δt. The rate $h_{\mathcal{P}}$ is the entropy per unit time of the partition $\mathcal{P}$ and the KS entropy is defined as [1, 5]

$$h_{\rm KS} = {\rm Sup}_{\mathcal{P}}\ h_{\mathcal{P}} \tag{32}$$

The KS entropy can equivalently be introduced in terms of the Chaitin-Kolmogorov-Solomonoff algorithmic complexity K_t, which is the length of the shortest program running on a universal Turing machine and able to reproduce the trajectory over a time interval t. The length of the program can be measured as the binary length or in the base of natural logarithms as assumed from now on. If the trajectory is periodic, it is enough to store the pattern of one period and the number of periods over the time t so that the length of this program grows as $\ln t$. However, if the trajectory is random there is no other mean than to store the whole segment of trajectory in which case the length of the program grows proportionally to the time t, which is the fastest possible growth. The growth rate of the algorithmic complexity is equal to the KS entropy

$$h_{\rm KS} = \lim_{t\to\infty} \frac{1}{t}\ K_t \tag{33}$$

for μ-almost all the trajectories [57]. This result shows that the KS entropy per unit time characterizes the dynamical randomness developed by the system during its time evolution.

A system is defined to be *chaotic* if it is deterministic (i.e., governed by a mapping or a differential equation) and its KS entropy per unit time is positive [3].

The KS entropy is related to the sum of positive Lyapunov exponents and the rate of escape γ of trajectories out of an open system according to a generalization of Pesin's theorem [1]

$$h_{\rm KS} = \sum_{\lambda_i>0} \lambda_i - \gamma \tag{34}$$

In closed systems, the escape rate vanishes $\gamma = 0$ and the KS entropy is given by the sum of positive Lyapunov exponents, which is the content of Pesin's theorem. If there exists at least one positive Lyapunov exponent the KS entropy is also positive and the time evolution is therefore random. In this case, we recover the usual definition of a chaotic system as a deterministic system with at least one positive Lyapunov exponent.

However, if the system is open, the dynamics can be nonchaotic if the escape rate is itself equal to the sum of positive Lyapunov exponents, $\gamma = \sum_{\lambda_i>0} \lambda_i$, because the KS entropy vanishes in this case. This situation happens in the system composed of a particle moving in a potential with a maximum, as well as in the two-disk scatterer where there is only one unstable periodic orbit which remains trapped at finite distance.

We notice that there exists the so-called *sporadic* systems which are intermediate between the periodic and the chaotic ones [3, 58]. In these systems, the trajectories have an algorithmic complexity which grows faster than the logarithm ($\ln t$) but slower than the time t, for instance as $t/(\ln t)$ or t^ν with $0 < \nu < 1$. Their KS entropy per unit time vanishes because the algorithmic complexity is not extensive in time. Nevertheless, the sporadic systems still develop a dynamical randomness but slower than in chaotic systems.

For deterministic systems with finitely many particles, the KS entropy is typically finite. However, the KS entropy may become infinite for systems with infinitely many particles. The extensivity of the entropy per unit time with the number of particles is an important issue in statistical mechanics. We can here define an entropy per unit time and per unit volume, which is positive if randomness is generated not only in time but also in space. If the particles do not interact as in an ideal gas or in a harmonic solid, the entropy per unit time and unit volume vanishes. On the other hand, this space-time entropy is positive in systems of interacting particles such as the hard-sphere gas [3]. The space-time entropy is also positive in probabilistic cellular automata [59–61], which therefore belong to the same class of random processes as the chaotic ones.

If the system is described as a random process generating continuously distributed variables, the KS entropy becomes infinite and no longer provides a useful characterization of the randomness. In this case, we should keep the notion of entropy per unit time associated with a partition into cells of diameter ε, defining in this way an ε-entropy per unit time [4]. Processes in which a finite number of outcomes of continuously distributed variables happens per unit time typically have their ε-entropy per unit time diverging as $\ln(1/\varepsilon)$ for $\varepsilon \to 0$. An example is the random processes described by the linearized Boltzmann equation which has an ε-entropy per unit time and unit volume diverging as $\ln(1/\varepsilon)$ for $\varepsilon \to 0$, although the deterministic Hamiltonian equations generate a random process with a finite entropy per unit time and unit volume [3, 4]. On the other hand, Langevin processes generate continuously distributed variables continuously in time, leading to an ε-entropy typically diverging as ε^{-2} for $\varepsilon \to 0$ [3, 4]. Langevin processes are thus qualitatively more random than the aforementioned processes.

The ε-entropy per unit time depends on the kind of boundary conditions which are considered. In finite systems with reflecting or periodic boundary conditions, the determinism is preserved throughout the whole time evolution so that the dynamical randomness is characterized by a finite KS entropy per unit time. If the system is in contact with reservoirs, the interaction of the particles with the walls is in general stochastic and described by a nondeterministic Langevin process in a thin boundary layer near the wall of the reservoir [49]. In this case, the process is characterized by an ε-entropy per unit time which can be estimated as $Vh^{(\text{time,volume})} + cA\varepsilon^{-2}$ where V and A are respectively the volume and area of the system, $h^{(\text{time,volume})}$ is the bulk entropy per unit time and unit volume, and c some constant characteristic of the Langevin process. If the stochastic layer has a negligible thickness with respect to the size of the system and if the contact with the reservoir is described by a flux boundary condition for Liouville's equation, the ε-entropy per unit time can be estimated as $Vh^{(\text{time,volume})} + \nu A \ln(1/\varepsilon)$ where ν is the frequency of income of new particles at the boundary (with the same notations as before). The logarithmic divergence of the ε-entropy per unit time results from the fact that each new incoming particle brings five continuously distributed random variables: two positions for the point of crossing with the wall and three velocities. The bulk entropy per unit time and unit volume $h^{(\text{time,volume})}$ can be estimated as the sum of positive Lyapunov exponents divided by the volume V for systems close to equilibrium: $h^{(\text{time,volume})} = 0$ for an ideal gas, while $h^{(\text{time,volume})} > 0$ for a hard-sphere gas. Accordingly, the dynamical randomness is dominated by the bulk dynamical instability in systems of interacting particles [3].

IV. MICROSCOPIC APPROACH TO THE DECAY AND RELAXATION OF CLASSICAL SYSTEMS

A. Pollicott-Ruelle resonances

In a mixing system, the time correlation functions decay to their stationary values. It is an important issue to characterize the decay and, if possible, to decompose the decay in terms of exponentials. In order to investigate this question, we must consider the time asymptotics of the average quantities ruled by the Frobenius-Perron operator, i.e., the long-time behavior of the statistical averages (17) before they practically reach their stationary values. Recent work has shown the remarkable result that exponential decays are compatible with Hamiltonian dynamical systems [3, 14–16]. Hamiltonian systems exist for which:

$$\langle A \rangle_t \simeq_{t \to +\infty} \langle A|\Psi_{\text{st}}\rangle \, \langle \tilde{\Psi}_{\text{st}}|f_0\rangle + \sum_j \exp(s_j t) \, \langle A|\Psi_j\rangle \, \langle \tilde{\Psi}_j|f_0\rangle + (\text{Jb}) \tag{35}$$

where s_j are the so-called Pollicott-Ruelle resonances [8–13] associated with the eigenstates

$$\hat{P}^t \Psi_j = \exp(s_j t) \, \Psi_j \tag{36}$$

$$\hat{P}^{t\dagger} \tilde{\Psi}_j = \exp(s_j^* t) \, \tilde{\Psi}_j \tag{37}$$

of the Frobenius-Perron operator $\hat{P}^t$ here considered as the evolution operator of the forward semigroup. Since the evolution operator of the semigroup is not unitary the resonances are in general complex and, moreover, there is the possibility of formation of Jordan blocks denoted by (Jb) in Eq. (35) [3]. Jordan-block structures arise from multiple

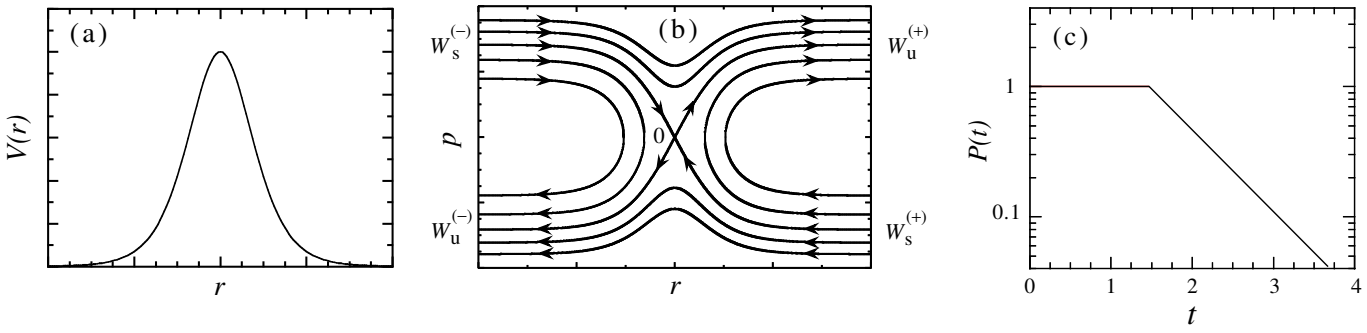

FIG. 5: Particle moving down a hill under the Hamiltonian (39): (a) the potential; (b) the phase portrait; (c) a typical survival probability versus time.

eigenvalues in the spectrum and lead to time behavior as $t^{m_j-1}\exp(s_j t)$ where m_j is the multiplicity of the resonance s_j. Jordan-block structures are not exceptional especially in Hamiltonian systems, but we shall here focus on the eigenstates.

In classical dynamical systems, the eigenstates Ψ_j or $\tilde{\Psi}_j$ are generally given by mathematical distributions so that the associated measures are singular contrary to what is usually assumed in kinetic theory. These singular measures can be constructed by a kind of semigroup renormalization obtained by rewritting Eq. (36) in the following form [3, 62]

$$\Psi_j = \lim_{t\to+\infty} \exp(-s_j t)\ \hat{P}^t \Psi_j \tag{38}$$

As a simple example of time asymptotics, let us consider a particle moving in a one-dimensional potential under the Hamiltonian

$$H = \frac{p^2}{2M} + V(r) \tag{39}$$

The potential $V(r)$ is supposed to have a unique maximum at $r = 0$ and to monotonously decrease to a constant value at large distances $r \to \pm\infty$ so that $V(0) > V(r) > V(+\infty) = V(-\infty)$ (see Fig. 5a). The phase space of this one-degree-of-freedom system is the plane of the variables $\Gamma = (r, p)$. The point $r = p = 0$ is an unstable fixed point of the flow. Two branches of unstable manifold are issued from the fixed point and are asymptotic to the momenta $p = \pm\sqrt{2M\,[V(0) - V(\infty)]}$ for $r \to \pm\infty$ respectively (see Fig. 5b). By time-reversal symmetry, there exist two branches of stable manifold of trajectories incoming from infinity and reaching asymptotically the fixed point as $t \to +\infty$. The stable and unstable manifolds form a separatrix between the low-energy trajectories which always remain on one side of the maximum and the high-energy trajectories which move from one side to the other. If the statistical ensemble of initial conditions is located around the fixed point, the number of trajectories which remain in the vicinity of the fixed point is observed to decay exponentially as $t \to +\infty$ (see Fig. 5c). The rate of decay is the so-called escape rate γ, which is equal to the Lyapunov exponent λ of the fixed point in this simple system. The reason for this equality is that the trajectories escaping after a long time are coming from very close to the maximum and their dynamics is controlled by the linear stability of the fixed point. This simple system thus provides an example of a nonchaotic system with a positive Lyapunov exponent but a vanishing KS entropy because $\gamma = \lambda$. We notice that the positivity of the Lyapunov exponent implies the exponential decay so that there is here a close connection between the hyperbolicity of the dynamics near the fixed point and the existence of an exponential decay. During the decay, the cloud of points tends to stretch along both branches of unstable manifold as $t \to +\infty$. Asymptotically in time, the statistical ensemble will be distributed as a kind of Dirac distribution having the branches $\{\Gamma_u^{(\epsilon)}\}_{\epsilon=\pm}$ of the unstable manifold for support. This intuition is supported by the fact that the following expression,

$$\Psi(\Gamma) \ = \ \sum_{\epsilon=\pm} \int_{-\infty}^{+\infty} \exp(\gamma\tau)\ \delta\left[\Gamma - \Gamma_u^{(\epsilon)}(\tau)\right]\ d\tau \tag{40}$$

defines an exact eigenstate of the Frobenius-Perron operator associated with the escape rate γ because

$$\hat{P}^t \Psi(\Gamma) \ = \ \Psi(\Phi^{-t}\Gamma) \ = \ \exp(-\gamma t)\ \Psi(\Gamma) \tag{41}$$

since the flow is area-preserving and $\Phi^t \Gamma_{\rm u}^{(\epsilon)}(\tau) = \Gamma_{\rm u}^{(\epsilon)}(\tau + t)$. This result shows that the leading Pollicott-Ruelle resonances of this simple system is essentially given by the escape rate: $s = -\gamma$ [3, 62].

A complete asymptotic expansion of statistical averages in terms of decaying exponential functions is given in Appendix A for the simple case of the inverted harmonic potential. Such complete asymptotic expansions have also been constructed in simple flows undergoing a pitchfork and a Hopf bifurcations [63, 64]. In these bifurcating systems, the spectrum of Pollicott-Ruelle resonances collapses onto a continuous spectrum at the bifurcation, leading to power-law decay at criticality.

Exponential relaxation to the invariant measure can also be proved in simple chaotic systems such as the baker map, as shown in Appendix B. Besides the simple models which are analytically tractable, the Pollicott-Ruelle resonances can be numerically obtained thanks to the periodic-orbit theory.

B. Periodic-orbit theory

The periodic-orbit theory of the classical systems is based on the Cvitanović-Eckhardt trace formula which expresses the trace of the Frobenius-Perron operator of the flow at energy E as a sum over the periodic orbits $\{p\}$ and their repetitions $r = 1, 2, 3, ...$

$$\mathrm{Tr}_E \, \mathrm{e}^{\hat{L}t} \equiv \int_E \delta(X - \Phi_E^t X) \, dX = \sum_p \sum_{r=1}^{\infty} T_p \, \frac{\delta(t - rT_p)}{|\det(\mathbf{I} - \mathbf{m}_p^r)|} \tag{42}$$

where X are the phase-space coordinates inside the energy shell, T_p is the prime period of the periodic orbit p, and $\mathbf{m}_p$ is the linearized Poincaré map evaluated on the periodic orbit [65].

The Laplace transform of the trace of the Frobenius-Perron operator is formally identical to the trace of the resolvent of the Liouvillian operator and it can be expressed in terms of the so-called classical Zeta function $Z_{\rm cl}$ for a hyperbolic dynamical system in which all the periodic orbits are isolated and unstable:

$$\int_0^\infty \mathrm{e}^{-st} \, \mathrm{Tr}_E \, \mathrm{e}^{\hat{L}t} \, dt = \mathrm{Tr}_E \, \frac{1}{s - \hat{L}} = \frac{\partial}{\partial s} \, \ln \, Z_{\rm cl}(s; E) \tag{43}$$

For a two-degree-of-freedom hyperbolic system, the classical Zeta function is a product over all the unstable periodic orbits:

$$Z_{\rm cl}(s; E) \; = \; \prod_p \prod_{m=0}^{\infty} \left\{ 1 \; - \; \frac{\exp\left[-sT_p(E)\right]}{|\Lambda_p(E)| \, \Lambda_p(E)^m} \right\}^{m+1} \tag{44}$$

where Λ_p is the (instability) eigenvalue of the linearized Poincaré map of the periodic orbit p. Since each periodic orbit is unstable we have that $|\Lambda_p| > 1$. The Pollicott-Ruelle resonances s_j are given as the zeros of the Zeta function:

$$Z_{\rm cl}(s_j; E) = 0 \tag{45}$$

The periodic-orbit theory has been applied to different systems in order to characterize the decay of a statistical ensemble of trajectories [14]. A class of systems which have been studied in detail are the disk scatterers.

In the two-disk scatterer, there is a single unstable periodic orbit bouncing between the two disks (see Fig. 6a). This unique periodic orbit forms the so-called repeller of this system, which is the set of trajectories which are forever trapped at finite distance. This periodic orbit has a positive Lyapunov exponent λ which is proportional to the velocity of the particle. The instability eigenvalue is given by $\Lambda = \exp(\lambda T)$ where T is the period which is inversely proportional to the velocity. The Pollicott-Ruelle resonances of the two-disk scatterer are the zeros of the Zeta function:

$$Z_{\rm cl}(s) \; = \; \prod_{m=0}^{\infty} \left[1 \; - \; \frac{\exp\left(-sT\right)}{|\Lambda| \, \Lambda^m} \right]^{m+1} = 0 \tag{46}$$

This infinite product converges absolutely so that the Pollicott-Ruelle resonances are given by

$$s_{mn} = -\frac{m+1}{T} \ln \Lambda + \mathrm{i} \, \frac{2\pi n}{T} \tag{47}$$

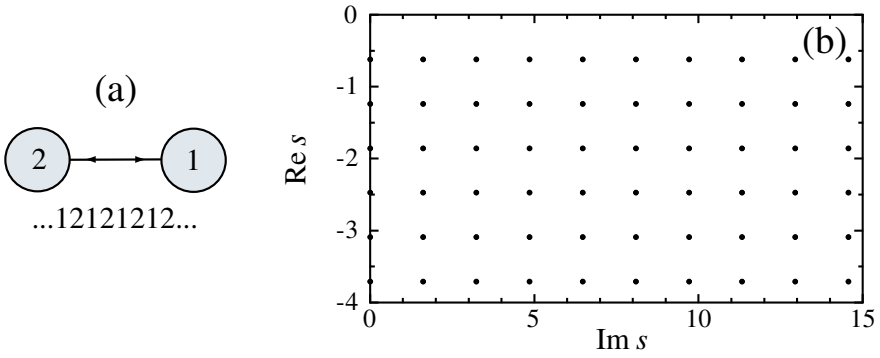

FIG. 6: Two-disk scatterer: (a) configuration of the system; (b) spectrum of Pollicott-Ruelle resonances.

with $m = 0, 1, 2, 3, ...$ and $n = 0, \pm 1, \pm 2, \pm 3, ...$ The resonances form a half periodic array extending toward negative values of Re s and separated from Re $s = 0$ by a gap given by the escape rate

$$\gamma = \frac{1}{T} \ln \Lambda = \lambda \tag{48}$$

which is here equal to the Lyapunov exponent (see Fig. 6b). Accordingly, the KS entropy vanishes and the system is nonchaotic as expected.

In order to obtain a chaotic system, it is enough to add a third disk forming an equilateral triangle with the two previous disks, which defines the three-disk scatterer (see Fig. 7a). In this open system, the set of trapped trajectories forms a fractal and chaotic repeller. If the disks are sufficiently far apart, the forever trapped trajectories are in one-to-one correspondence with a symbolic dynamics based on the labels of the disks with the constraint that no two consecutive labels are equal because the particle cannot bounce twice on the same disk without having an intermediate collision on another disk [20]. This constraint means that the symbolic dynamics is effectively dyadic, leading to a twofold proliferation of orbits with the period. All the periodic orbits can be listed in order of increasing period or instability. This listing helps to numerically compute the Zeta function by truncation after a given period, which amounts to neglect the effect of the most unstable trajectories. This method, called the cycle expansion [66], is excellent in a system such as the three-disk scatterer and allows a high-precision calculation of the different characteristic quantities of chaos with four or five digits [14]. In particular, it is possible to calculate the spectrum of Pollicott-Ruelle resonances (see Fig. 7b). Because of the threefold symmetry of the equilateral three-disk scatterer the Pollicott-Ruelle resonances fall into the different irreducible representations (A_1, A_2, and E) of the C_{3v} symmetry group. The spectrum is separated from the imaginary axis by a gap given by the escape rate γ which is the leading Pollicott-Ruelle resonances. Since the system is chaotic, the escape rate is no longer equal to the maximum Lyapunov exponent but it is lowered by the KS entropy per unit time according to: $\gamma = \lambda - h_{\rm KS}$. The different Pollicott-Ruelle resonances control the decay of a statistical ensemble of trajectories escaping from the scatterer. The survival probability, i.e., the probability that a trajectory is still in the vicinity of the scatterer, decays in a gross exponential way at a rate given by the escape rate. But on top of the decay curve, we observe modulations at certain frequencies which are precisely given by the imaginary parts of the Pollicott-Ruelle resonances (see Figs. 7c and 7d) [14].

This phenomenon is also clearly evidenced in Fig. 8 which depicts the survival probability in two geometries of the four-disk scatterer, composed of four disks forming a square of side $R = 12$ and $R = 24$ respectively, the radius of the disks being taken as unity. In these systems, the modulations of the survival probability are very pronounced and their Fourier transform presents peaks at the frequencies of the Pollicott-Ruelle resonances as can be seen in Fig. 8 [14]. These results show that the Pollicott-Ruelle resonances control the decay under classical dynamics in these open systems.

C. Escape-rate theory of transport

The purpose of the escape-rate theory of transport is to express the transport coefficients in terms of the escape rate of some fractal repeller [3, 17–19]. The fractal repeller is defined by considering some absorbing boundary conditions in the phase space of the system. The absorbing boundary conditions set up a first passage problem for the Liouvillian equation ruling the time evolution of the statistical ensemble of trajectories. As explained here above, the probability density $f(\Gamma)$ evolves in time according to Liouville's equation. Since this latter is a partial differential equation, it

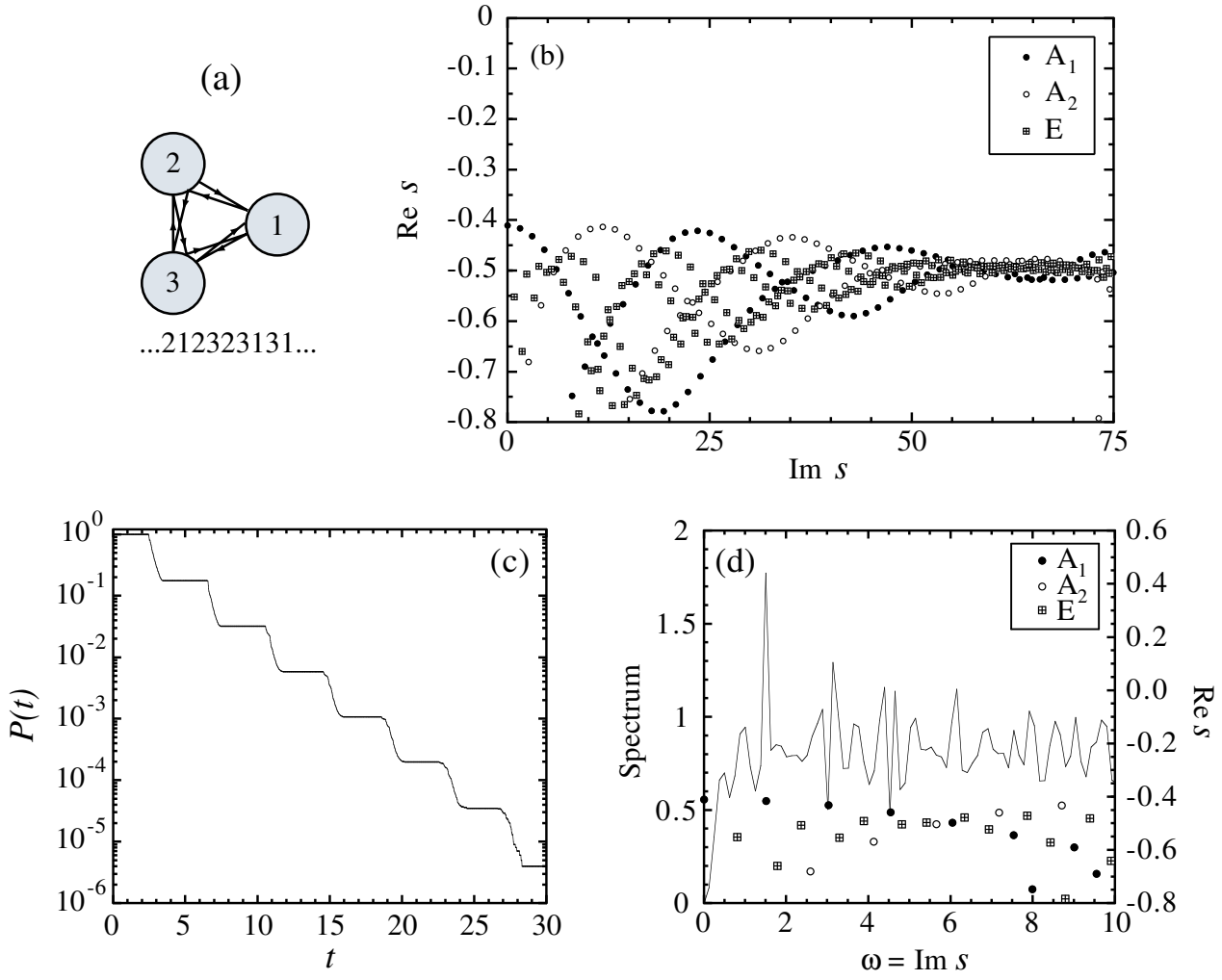

FIG. 7: Three-disk scatterer: (a) configuration of the system; (b) spectrum of Pollicott-Ruelle resonances; (c) typical survival probability versus time; (d) Fourier transform of the modulations of the survival probability versus the frequency, compared with the spectrum of Pollicott-Ruelle resonances.

requires boundary conditions to be solved. The absorbing boundary conditions impose that there is a vanishing flux of incoming trajectories at the border of the system so that the probability (19) defines the survival probability and decays monotonously according to Eq. (25).

In general, the decay can be a power law (possibly corrected by logarithms) or an exponential. In finite ergodic hyperbolic systems with positive Lyapunov exponents, the decay turns out to be exponential in the long-time limit $t \to \infty$ with a positive escape rate related to the positive Lyapunov exponents and the KS entropy according to Eq. (34). The set of trapped trajectories form a fractal and chaotic repeller, which can be characterized in terms of the partial information dimensions $\{d_i\}$ associated with the different unstable directions in phase space [1]

$$h_{\rm KS} = \sum_{\lambda_i > 0} d_i \, \lambda_i \tag{49}$$

The codimensions are defined by $c_i = 1 - d_i$ so that the escape rate can be written in terms of the positive Lyapunov exponents and the partial codimensions as [1]

$$\gamma = \sum_{\lambda_i > 0} \lambda_i - h_{\rm KS} = \sum_{\lambda_i > 0} c_i \, \lambda_i \tag{50}$$

The transport properties such as diffusion, viscosity or heat conductivity are characterized by coefficients which enter the macroscopic equations of motion such as the diffusion or heat equations and the Navier-Stokes equations. In

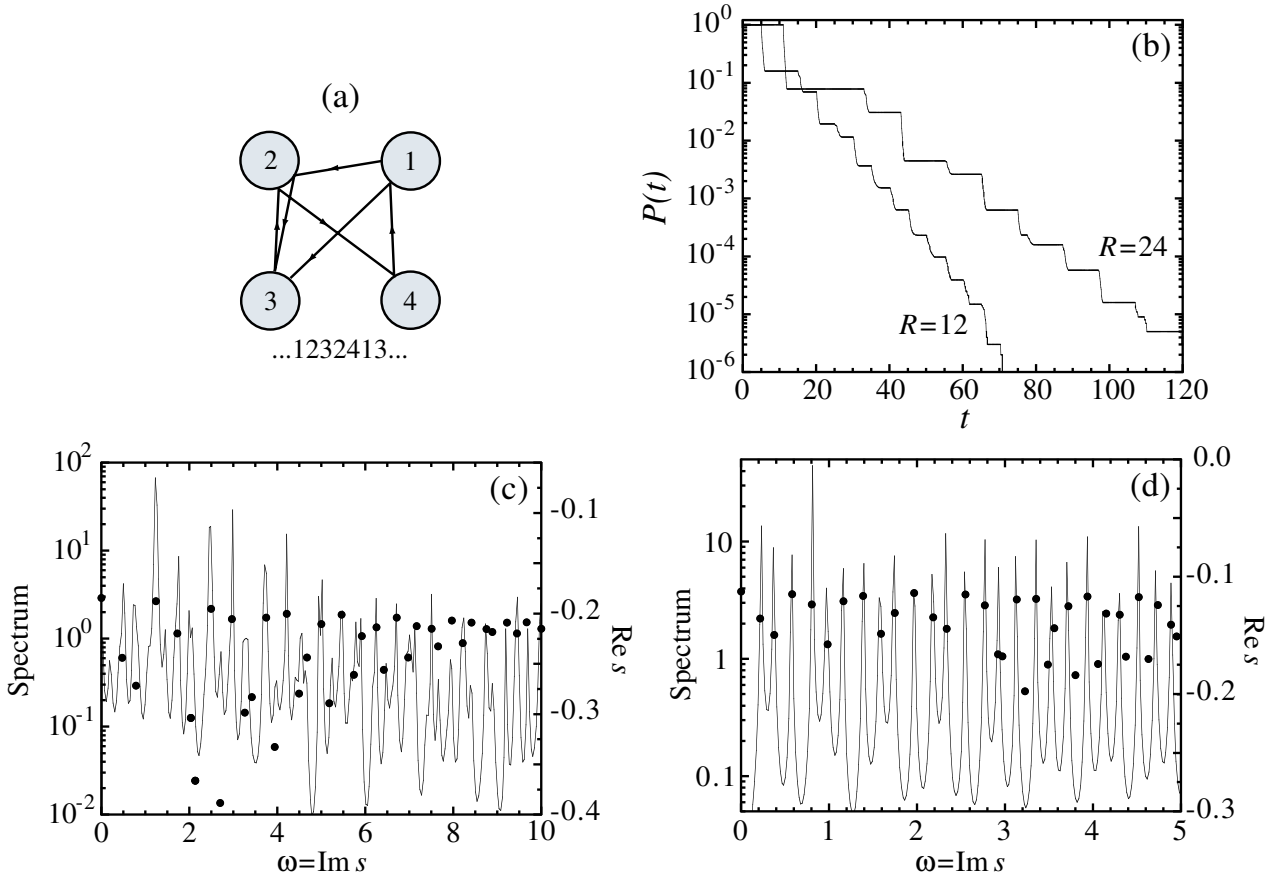

FIG. 8: Four-disk scatterer composed of four disks of unit radius at the vertices of a square of size R: (a) configuration of the system; (b) survival probabilities versus time for the configurations with $R = 12$ and $R = 24$; (c) Fourier transform of the modulations of the survival probability versus the frequency, compared with the spectrum of Pollicott-Ruelle resonances in the case $R = 12$ and (d) in the case $R = 24$.

the fifties and early sixties, these transport coefficients have been expressed in terms of the Helfand moments $G^{(\alpha)}$ or the microscopic currents $J^{(\alpha)} = dG^{(\alpha)}/dt$ [6, 7, 67]. In particular, the transport coefficients are given as the integral of the time autocorrelation function of each microscopic current by the Green-Kubo formula [6, 7] or, equivalently, as the linear growth rate of the variance of the Helfand moment [67]

$$\alpha = \int_0^\infty \langle J_0^{(\alpha)} J_t^{(\alpha)} \rangle \, dt = \lim_{t\to\infty} \frac{1}{2t} \, \langle (G_t^{(\alpha)} - G_0^{(\alpha)})^2 \rangle \tag{51}$$

The Helfand moments associated with the different transport properties are given in Table I.

The Einstein-like formula in Eq. (51) shows that the Helfand moments have a diffusive motion. A first passage problem can be set up by imposing absorbing boundary conditions in the space of variation of the Helfand moment [18]. These absorbing boundary conditions select all the trajectories of the whole system for which the Helfand moment never reaches the absorbing boundaries:

$$-\frac{\chi}{2} \leq G_t^{(\alpha)} \leq +\frac{\chi}{2} \tag{52}$$

However, most of the trajectories reach the absorbing boundaries and escape out of the domain delimited by these boundaries. Accordingly, the trajectories forever trapped inside the absorbing boundaries form a set of zero probability in the form of a fractal repeller. This repeller is characterized by an escape rate which can be evaluated by using the equation of diffusive motion of the Helfand moment $g = G_t^{(\alpha)}$

$$\frac{\partial p}{\partial t} = \alpha \, \frac{\partial^2 p}{\partial g^2} \tag{53}$$

with the corresponding absorbing boundary conditions $p(g=\pm\chi/2,t)=0$. The solution of this equation is given by

$$p(g,t)=\sum_{j=1}^{\infty} a_j\ \exp(-\gamma_j t)\ \sin\left(\frac{j\pi g}{\chi}+\frac{j\pi}{2}\right) \tag{54}$$

so that the decay rates of the survival probability are

$$\gamma_j=\alpha\left(\frac{j\pi}{\chi}\right)^2 \qquad \text{and} \quad j=1,2,3,... \tag{55}$$

The escape rate is the slowest decay rate which is thus related to the transport coefficient α according to

$$\gamma\simeq\gamma_1=\alpha\left(\frac{\pi}{\chi}\right)^2 \qquad \text{for} \quad \chi\to\infty \tag{56}$$

Substituting this result in the escape-rate formula (50) we obtain the following relationships between the transport coefficients and the characteristic quantities of chaos which are the Lyapunov exponents λ_i, the KS entropy $h_{\rm KS}$, or the partial codimensions c_i as [18]

$$\alpha\ =\ \lim_{\chi,V\to\infty}\left(\frac{\chi}{\pi}\right)^2\left(\sum_{\lambda_i>0}\lambda_i-h_{\rm KS}\right)_\chi\ =\ \lim_{\chi,V\to\infty}\left(\frac{\chi}{\pi}\right)^2\left(\sum_{\lambda_i>0}c_i\ \lambda_i\right)_\chi \tag{57}$$

In the limit $\chi\to\infty$, the partial information codimensions can be replaced by the Hausdorff codimensions in hyperbolic systems.

TABLE I. Helfand's moments of different transport properties.

transport property	*moment*
self-diffusion	$G^{(\mathcal{D})}\ =\ x_i$
shear viscosity	$G^{(\eta)}\ =\ \frac{1}{\sqrt{Vk_{\rm B}T}}\ \sum_{i=1}^{N}\ x_i\ p_{iy}$
bulk viscosity ($\psi=\zeta+\frac{4}{3}\eta$)	$G^{(\psi)}\ =\ \frac{1}{\sqrt{Vk_{\rm B}T}}\ \sum_{i=1}^{N}\ x_i\ p_{ix}$
heat conductivity	$G^{(\kappa)}\ =\ \frac{1}{\sqrt{Vk_{\rm B}T^2}}\ \sum_{i=1}^{N}\ x_i\ (E_i\ -\ \langle E_i\rangle)$
electric conductivity	$G^{(\rm e)}\ =\ \frac{1}{\sqrt{Vk_{\rm B}T}}\ \sum_{i=1}^{N}\ eZ_i\ x_i$

Equation (57) has been applied to the transport by diffusion in the open two-dimensional periodic Lorentz gas (see Fig. 9a) [68]. In this system, the particles have a deterministic diffusive motion induced by the elastic collisions on immobile scatterers until the particles escape upon reaching absorbing boundaries in the form of a hexagon, a circle, or two parallel lines separated by a large distance L. The absorbing boundary conditions select a fractal repeller of trapped trajectories which can be numerically evidenced by plotting the time to escape as a function of initial condition (see Fig. 9b). In this two-degree-of-freedom system, there is only one unstable direction and, thus, one positive Lyapunov exponents and associated codimension. Accordingly, Eq. (57) shows that the diffusion coefficient is given by [17, 68]

$$\mathcal{D}\ =\ \lim_{L\to\infty}\left(\frac{L}{\pi}\right)^2\ (\lambda-h_{\rm KS})_L\ =\ \lim_{L\to\infty}\left(\frac{L}{\pi}\right)^2\ (c\ \lambda)_L \tag{58}$$

where c is either the information or the Hausdorff partial codimension associated with the unstable direction. The open random Lorentz gases have also been investigated [69].

The escape-rate theory has also been applied to reaction-diffusion processes in which point particles diffuse in a Lorentz gas until they reach catalytic disks where they are annihilated [70]. In this reactive process, absorbing boundary conditions are set up on the border of the catalytic disks and select a fractal repeller of trajectories which

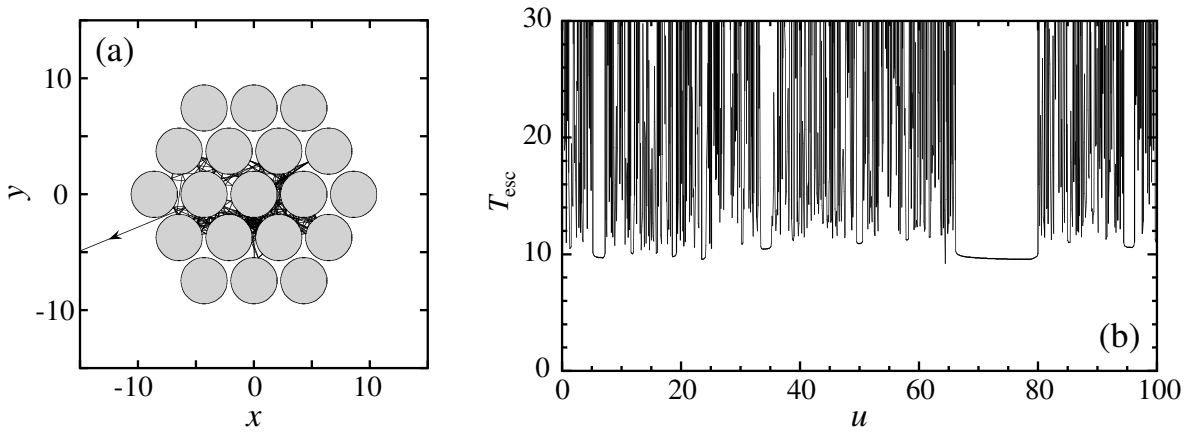

FIG. 9: Open Lorentz gas: (a) configuration of the system with a typical trajectory; (b) time taken by the particle to escape versus the initial angle $\theta = 0.75\pi - u\pi 10^{-10}$ of velocity of the particle starting from the central disk. The escape time becomes infinite on each stable manifold of a trapped trajectory.

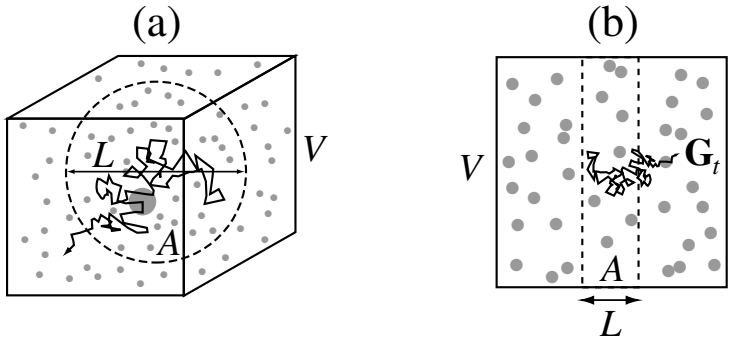

FIG. 10: Schematic illustration of the application of the escape-rate theory to (a) the diffusion of a Brownian particle escaping out of a sphere A of diameter L in a fluid of volume V and (b) the viscosity in a fluid of volume V in which the Helfand moment $\mathbf{G}_t$ escapes out of a domain A of width L.

never hit a catalyst. In this reaction-diffusion system, the reaction rate is given by the escape rate, which is in turn related to the characteristic quantities of chaos [70].

Equation (57) can also be applied to transport in many-body systems such as the diffusion of a Brownian or tracer particle in a fluid of other particles or to the shear viscosity (see Fig. 10). In these many-body systems, there is a spectrum of Lyapunov exponents as well as of partial codimensions. Typically, the spectrum of codimensions is peaked on the maximum Lyapunov exponent in multidimensional fractal repellers.

The escape-rate theory can also be considered for the determination of the mobility coefficient in the biased diffusion of a charged particle in a static external electric field [3, 71], or for heating by the diffusivity of total energy in systems driven by a time-periodic external force.

D. Hydrodynamic and reactive modes in spatially extended systems

In spatially extended systems, the relaxation to the equilibrium state is ruled by the hydrodynamic modes. These modes can be explicitly constructed in periodic dynamical systems which are spatially extended by considering infinitely many images of the system in the form of a checkerboard [72–74].

A simple example is the periodic Lorentz gas in which the unit cell contains a single scatterer. The system is spatially extended by tessellating the plane with the unit cell. The motion of the point particle bouncing on the disk can be considered either inside the unit cell which forms a torus, or in the array formed by the infinitely many images of the unit cell. Diffusion is conceived as the irregular motion on the infinite spatially extended system. When the particle performs a bounded chaotic motion inside the unit cell (or torus) its images diffuses on the lattice made

of the infinitely many images of the unit cell. The probability density of finding the particle on the lattice can be Fourier transformed and decomposed into different components associated with the different values of the wavenumber $\vec{k}$ ranging in the first Brillouin zone of the lattice. Each $\vec{k}$-component of the probability density has its own time evolution under an operator $\hat{Q}^t_{\vec{k}}$ which is obtained by Fourier transforming the Frobenius-Perron operator $\hat{P}^t$ over the whole lattice. This new operator may admit Pollicott-Ruelle resonances which also depend on the wavenumber as for the associated eigenstates:

$$\hat{Q}^t_{\vec{k}}\ \Psi_{\vec{k}} = \mathrm{e}^{s_{\vec{k}}t}\ \Psi_{\vec{k}} \tag{59}$$

If $\hat{T}^{\vec{l}}$ denotes the operator of translation by the lattive vector $\vec{l}$, the eigenstates satisfy the *quasiperiodic boundary conditions*:

$$\hat{T}^{\vec{l}}\ \Psi_{\vec{k}} = \mathrm{e}^{\mathrm{i}\vec{k}\cdot\vec{l}}\ \Psi_{\vec{k}} \tag{60}$$

When the wavenumber vanishes $\vec{k} = 0$, we recover the Frobenius-Perron operator only ruling the dynamics on the torus. If this dynamics is ergodic and mixing as it is the case for the Lorentz gas or the Sinai billiard one of the Pollicott-Ruelle resonances must be identical to the vanishing Liouvillian eigenvalue $s_0 = 0$ associated with the unique invariant measure. This suggests that, at least, one of the Pollicott-Ruelle resonances vanishes with the wavenumber: $\lim_{\vec{k}\to 0} s_{\vec{k}} = 0$. Since the Pollicott-Ruelle resonances rule the relaxation to the invariant measure we can identify that particular Pollicott-Ruelle resonance with the dispersion relation of the hydrodynamic mode of diffusion [3, 72]. This dispersion relation is given by the van Hove formula as [73]

$$s_{\vec{k}} = \lim_{t\to\infty} \frac{1}{t} \ln\langle \exp[\mathrm{i}\vec{k}\cdot(\vec{r}_t - \vec{r}_0)]\rangle = -\mathcal{D}\ k^2 + O(k^4) \tag{61}$$

which is a consequence of Eqs. (59) and (60).

At the microscopic level of description, the hydrodynamic mode is thus represented by the corresponding eigenstate (59) of the evolution operator. This eigenstate is typically a mathematical distribution represented by a cumulative function which is continuous but nondifferentiable.

In two-degree-of-freedom systems such as the two-dimensional Lorentz gases, the cumulative functions of the hydrodynamic modes of diffusion can be defined in terms of the density $\Psi_{\vec{k}}$ of the eigenstate as the one-dimensional integral over a line in phase space

$$F_{\vec{k}}(\xi) = \int_0^\xi d\xi'\ \Psi_{\vec{k}}(\Gamma_{\xi'}) \tag{62}$$

For $\vec{k} \neq 0$, this function is complex and forms a fractal curve in the complex plane (see Fig. 11) [73]. Its Hausdorff dimension depends on the wavenumber $\vec{k}$, the diffusion coefficient $\mathcal{D}$, and the positive Lyapunov exponent λ as [73, 75]

$$D_{\mathrm{H}}(\vec{k}) = 1 + \frac{\mathcal{D}}{\lambda}\ k^2 + O(k^4) \tag{63}$$

This formula can be rewritten to express the diffusion coefficient in terms of the Hausdorff dimension and the other characteristic quantities of chaos as [73, 75]

$$\mathcal{D} = \lim_{\vec{k}\to 0} \left(\frac{1}{k}\right)^2 \Big[\lambda\ (D_{\mathrm{H}} - 1)\Big]_{\vec{k}} \tag{64}$$

which has a structure very similar to the escape-rate formula (58). Indeed, in the problem with absorbing boundary conditions, the role of the wavenumber is played by $k = \pi/L$, the Lyapunov exponent is essentially the same for both problems in the limits $L \to \infty$ or $\vec{k} \to 0$ in which the Lyapunov exponent reaches the value obtained by averaging over the equilibrium invariant measure. On the other hand, the partial Hausdorff codimension of the fractal repeller is given by $c_{\mathrm{H}} = 1 - d_{\mathrm{H}}$ which is positive since the Hausdorff dimension of a fractal object on a line is known to be bounded as $0 \leq d_{\mathrm{H}} \leq 1$. The role of the partial Hausdorff dimension of the repeller is here played by the Hausdorff dimension of the fractal cumulative curve in the two-dimensional complex plane, which is bounded as $1 \leq D_{\mathrm{H}} \leq 2$. We therefore find the positive number $D_{\mathrm{H}} - 1$ in Eq. (64) in the place of the codimension c appearing in Eq. (58).

The hydrodynamic modes have been explicitly constructed and shown to have fractal cumulative functions in the hard-disk and Yukawa potential Lorentz gases [73], as well as in the multibaker model of diffusion (see Appendix C). Similar considerations apply to the reactive modes of reaction-diffusion processes in which colored particles diffuse in a Lorentz gas and change their color upon colliding on catalytic disks [40–42]. The reaction is here an isomerization $A \leftrightarrow B$. The microscopic analysis of this reaction allows us to explicitly construct the diffusive and reactive modes of relaxation toward the thermodynamic equilibrium. These modes have fractal cumulative functions and their dispersion relations obey the macroscopic equations (4)-(8).

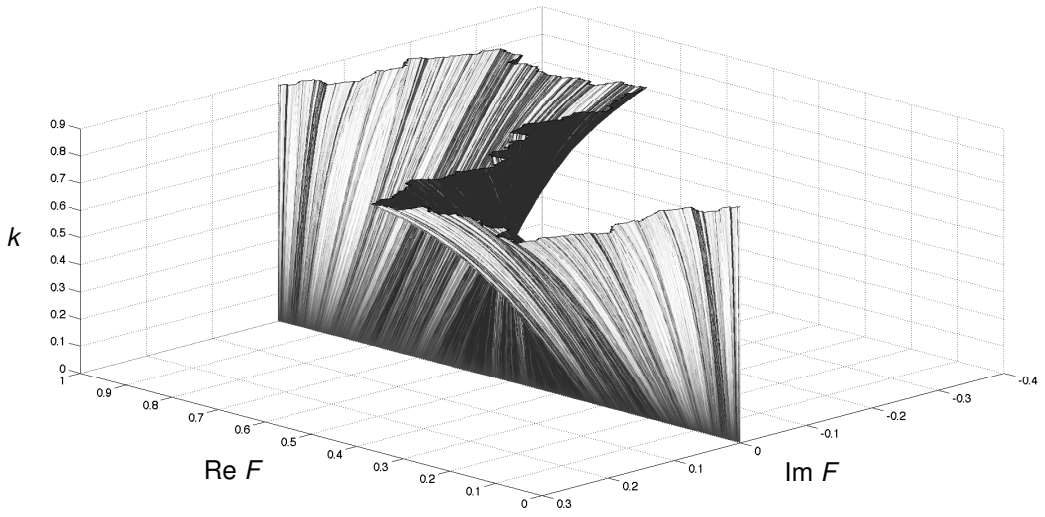

FIG. 11: Cumulative functions of the hydrodynamic modes of diffusion in the hard-disk Lorentz gas. The disks form a triangular lattice, their centers are separated by the distance $d = 2.3$, and their radius is unity. The cumulative functions (62) are depicted in the complex plane ($\mathrm{Re}\ F_{\vec{k}}, \mathrm{Im}\ F_{\vec{k}}$) versus their wavenumber $\vec{k} = k\ \vec{e}_x$ of magnitude varying in the interval $0 \leq k < 0.9$. ξ is here the angle of position on the border of a disk. The thermodynamic equilibrium corresponds to the vanishing wavenumber $k = 0$.

E. Explicit construction of a nonequilibrium steady state

The nonequilibrium steady state can be explicitly constructed in systems of diffusion between two reservoirs at different concentrations [3, 76]. To fix the idea, let us consider the open periodic Lorentz gas with flux boundary conditions at both sides separated by a distance L. From the left-hand side (resp. right-hand side), particles are incoming from a reservoir of phase-space density f_- (resp. f_+). The particle moves under the deterministic dynamics of elastic collisions inside the Lorentz gas. We suppose that the density has reached its stationary value between both reservoirs. At each point inside the Lorentz gas, the stationary density can then be determined by integrating the trajectory issued from this point backward in time till the point of entrance in the domain between both reservoirs. The density is f_- (resp. f_+) if the point of entrance is at the boundary with the left-hand side (resp. right-hand side) reservoir [76]. We notice that the backward integration can run for $t \to -\infty$ between both reservoirs in the case where the point belongs to the unstable manifold of one trapped trajectory of the fractal repeller of the escape-rate theory. Accordingly, the stationary density is a piecewise constant function taking the values f_+ or f_-. The discontinuities of the stationary density occurs on the unstable manifolds of the fractal repeller. This invariant density can be expressed by the formula

$$f_{\rm st}(\Gamma) \ = \ \frac{f_+ + f_-}{2} + \vec{g} \cdot \left[\vec{r}(\Gamma) + \int_0^{T_{\rm in}(\Gamma)} \vec{v}(\Phi^t \Gamma)\ dt \right] \tag{65}$$

where $T_{\rm in}(\Gamma)$ is the negative time of entrance of the trajectory going through the point Γ and $\vec{g} = \vec{e}_x (f_+ - f_-)/L$ is the gradient of phase-space concentration here taken in the x-direction. Indeed, if we integrate the velocity from the initial time $t = 0$ backward to the time of entrance, we get

$$f_{\rm st}(\Gamma) \ = \ \frac{f_+ + f_-}{2} + \vec{g} \cdot \Big[\vec{r}(\Gamma) + \vec{r}_{\rm in}(\Gamma) - \vec{r}(\Gamma) \Big] \tag{66}$$

Since the position of entrance is $\vec{r}_{\rm in} = \vec{e}_x(\pm L/2)$, we finally obtain that

$$f_{\rm st}(\Gamma) \ = \ \frac{f_+ + f_-}{2} + \frac{f_+ - f_-}{L}\ \frac{\pm L}{2} = f_\pm \tag{67}$$

as announced. The three terms in Eq. (65) can be interpreted as follows: The first term is simply the concentration in the middle of the system which is a constant. The second term represents the average linear profile of concentration

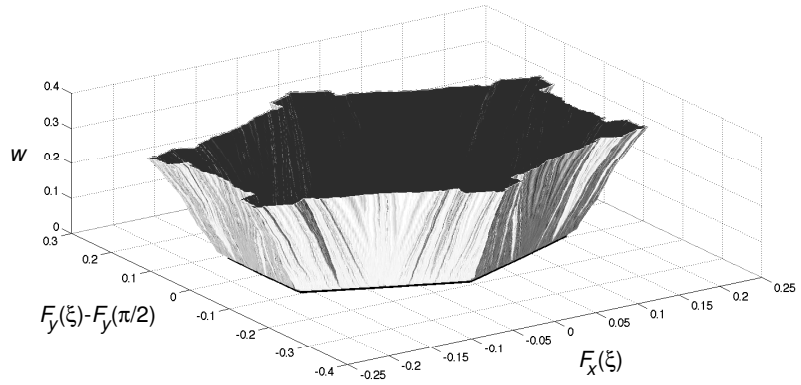

FIG. 12: Cumulative functions of the nonequilibrium steady states of diffusion in the hard-disk Lorentz gas. The scatterers are disks of unit radius forming a triangular lattice and separated by the gap w. The gap takes the values $0 \leq w < (4/\sqrt{3}) - 2$ in the finite-horizon case. In Eq. (70), ξ is the angle of position on the border of a disk and the gradient $\vec{g}$ is either in the x-direction or in the y-direction. The cumulative functions are depicted in the plane of the quantities $F_x(\xi)$ and $F_y(\xi) - F_y(\pi/2)$ versus the gap w between the disks.

expected for the nonequilibrium steady state of a diffusive system. It is remarkable that this linear profile arises simply from this formula. The third term represents the velocity fluctuations of deterministic origin around the mean linear profile.

In the limit where the reservoirs are at large distances while keeping the gradient of concentration constant, the stationary density in the middle of the system becomes wildely fluctuating between the concentrations of both reservoirs. The density relative to the average density is no longer defined as a function and becomes a distribution defined by a singular measure of invariant density

$$\Psi_{\vec{g}}(\Gamma) \; = \; \vec{g} \cdot \left[\vec{r}(\Gamma) + \int_0^{-\infty} \vec{v}(\Phi^t \Gamma) \; dt \right] = \Psi_{\vec{g}}(\Phi^t \Gamma) \tag{68}$$

It is remarkable that the invariant density (68) is equivalently obtained in terms of the hydrodynamic modes by considering the following zero wavenumber limit [3, 76]

$$\Psi_{\vec{g}}(\Gamma) \; = \; -\mathrm{i} \; \vec{g} \cdot \frac{\partial \Psi_{\vec{k}}(\Gamma)}{\partial \vec{k}} \Big|_{\vec{k}=0} \tag{69}$$

as shown elsewhere [77].

As for the hydrodynamic modes, the invariant density (68) is singular and the nonequilibrium steady state should be represented by its cumulative function as

$$F_{\vec{g}}(\xi) = \int_0^{\xi} d\xi' \; \Psi_{\vec{g}}(\Gamma_{\xi'}) \tag{70}$$

In the Lorentz gases and the multibaker models of diffusion, this cumulative function has been shown to be continuous but nondifferentiable [72, 77]. In the multibaker models of diffusion, this function is known as the Takagi function in the name of the Japanese mathematician who invented this function in 1903 as an example of continuous but nondifferentiable function [77]. In the Lorentz gases, the Takagi function generalizes into similar functions representing, at the microscopic phase-space level, the nonequilibrium steady states of diffusion corresponding to a linear average profile of concentration between both reservoirs (see Fig. 12) [62]. The singular character of the nonequilibrium steady states has very simply its origin in the mixing property of the deterministic dynamics which has the effect of mixing the different concentrations coming from both reservoirs.

F. Connection to thermodynamics

The connection between dynamics and thermodynamics has always been a difficult problem for the reason that many different irreversible processes take place in a fluid as explained in Sec. II. Progress in the theoretical understanding

has always proceeded by the analysis of simplified models such as the Ising model to understand critical phenomena in phase transitions. In the study of irreversible processes, the Lorentz gases and the multibaker models play a similar role because they only sustain one transport process, namely, diffusion. The Lorentz gas model has historically been introduced by Lorentz in 1905 as a model for transport of electrons in a solid [78]. Today, the Lorentz gas is considered as a model of diffusion of light particles among heavy ones [79, 80]. The heavy particles are immobile on the time scale of motion of the light particles. At each elastic collision between light and heavy particles, energy is nearly conserved although momentum is not. Therefore, the randomization of the velocity direction is very fast albeit the randomization of energy occurs on a much longer time scale. This decoupling of time scales does not preclude the existence of a well-defined diffusion coefficient on each energy shell. Indeed, Bunimovich and Sinai proved in 1980 that the two-dimensional hard-disk periodic Lorentz gas has a positive and finite diffusion coefficient if the horizon is finite, i.e., if no trajectory exists running through the lattice of hard disks without elastic collision [81]. Besides, the hard-disk Lorentz gas is ergodic and mixing. Similar results have been proved by Knauf for the two-dimensional periodic Lorentz gas composed of scatterers with Yukawa potentials under the condition that the energy of the moving particle is large enough [82]. The mixing property holds on each energy shell and leads to the establishment of a *local equilibrium in velocity direction*. The dynamics of elastic collision on the scatterers has the effect of randomizing the velocity *direction* so that the velocity distribution asymptotically becomes uniform in the *velocity angle*. This local equilibrium is sufficient for a transport by diffusion to occur which is compatible with the laws of irreversible thermodynamics.

In the perspective of Sec. II, the Lorentz gases are binary fluids composed of light particles diffusing among heavy particles which remain immobile. It is enough that the light particles interact with the heavy ones in order to induce diffusion. The interaction among the light particles is therefore neglected in the Lorentz gases. The light particles thus constitute a noninteracting gas of particles moving in a nonuniform potential due to the immobile heavy particles. This potential is such that the motion of each light particle is chaotic. This chaotic dynamics is mixing and induces the relaxation to the local equilibrium in the velocity direction as well as the diffusion across the lattice. On large spatial scales, the diffusion occurs on each energy shell so that the density $p(\vec{r},\epsilon)$ of light particles with energy ϵ at position $\vec{r}$ obeys the diffusion equation

$$\partial_t\, p(\vec{r},\epsilon) \simeq \mathcal{D}(\epsilon)\ \nabla^2 p(\vec{r},\epsilon) \tag{71}$$

where $\mathcal{D}(\epsilon)$ is the diffusion coefficient on the shell of energy ϵ [83]. At each elastic collision energy is conserved so that the initial distribution of energy is preserved by the dynamics. According to the zeroth law of thermodynamics, the temperature T of a system is fixed by putting it in contact with a heat reservoir before further operation. The implementation of the zeroth law of thermodynamics thus fixes the energy distribution of the ideal gas of light particles to a Boltzmann distribution at the given temperature which is thereafter invariant under the dynamics of the Lorentz gas. The large-scale density is thus given by

$$p(\vec{r},\epsilon) = n(\vec{r})\ \frac{\mathrm{e}^{-\epsilon/k_{\mathrm{B}}T}}{\int_0^\infty \mathrm{e}^{-\epsilon/k_{\mathrm{B}}T}\ d\epsilon} \tag{72}$$

where $n(\vec{r})$ is the number of particles per unit volume around the spatial point $\vec{r}$. The particle density $n(\vec{r})$ obeys the diffusion equation

$$\partial_t n(\vec{r}) \simeq \bar{\mathcal{D}}\ \nabla^2 n(\vec{r}) \tag{73}$$

with the mean diffusion coefficient

$$\bar{\mathcal{D}} = \frac{\int_0^\infty \mathrm{e}^{-\epsilon/k_{\mathrm{B}}T}\mathcal{D}(\epsilon)\ d\epsilon}{\int_0^\infty \mathrm{e}^{-\epsilon/k_{\mathrm{B}}T}\ d\epsilon} \tag{74}$$

The equilibrium thermodynamics of the hard-disk Lorentz gas is established as follows. Let us consider a gas of N noninteracting light particles in a spatial domain $\mathcal{Q}$ delimited by the hard disks and by a wall enclosing the Lorentz gas in a square. The volume of the domain $\mathcal{Q}$ is $V = \mathrm{Vol}(\mathcal{Q})$. The phase space of this gas is

$$\mathcal{M} = \left\{(\vec{r}_1,\vec{p}_1,...,\vec{r}_N,\vec{p}_N)|\vec{r}_i \in \mathcal{Q}, \vec{p}_i \in \mathbb{R}^d, x_1 < x_2 < \cdots < x_N\right\} \tag{75}$$

where the last conditions provide the ordering of indices required in the case of identical particles. The phase-space volume element is

$$d\Gamma = d\vec{r}_1\ \cdots\ d\vec{r}_N\ d\vec{p}_1\ \cdots\ d\vec{p}_N \tag{76}$$

and the invariant distribution is given in terms of the Maxwellian velocity distribution at the temperature T fixed by the zeroth law of thermodynamics:

$$f(\Gamma) = \frac{N!}{V^N} \frac{\exp\left(-\sum_{j=1}^{N} \frac{\vec{p}_j^{\,2}}{2mk_{\mathrm{B}}T}\right)}{(2\pi m k_{\mathrm{B}} T)^{Nd/2}} \tag{77}$$

which is normalized according to

$$\int_{\mathcal{M}} f(\Gamma)\, d\Gamma = 1 \tag{78}$$

The entropy can be calculated as Gibbs' coarse-grained entropy

$$S = -k_{\mathrm{B}} \sum_i p_i \ln p_i \tag{79}$$

by coarse graining the phase space into cells of size $\Delta\Gamma = \Delta^{Nd} r\, \Delta^{Nd} p = (2\pi\hbar)^{Nd}$. The probability for the system to belong to the i^{th} cell is

$$p_i = \int_{i^{\mathrm{th}}\ \mathrm{cell}} f\, d\Gamma \simeq f_i\, \Delta\Gamma \tag{80}$$

so that

$$S \simeq k_{\mathrm{B}} \left\langle \ln \frac{1}{f(\Gamma)\, \Delta\Gamma} \right\rangle \tag{81}$$

and we obtain the Sackur-Tetrode formula

$$S \simeq k_{\mathrm{B}}\, N\, \ln \frac{V \mathrm{e}^{\frac{d+2}{2}} (2\pi m k_{\mathrm{B}} T)^{\frac{d}{2}}}{N\, (2\pi\hbar)^d} \tag{82}$$

in the limit $N, V \to \infty$ keeping the particle density $n = N/V$ constant [84, 85]. This result shows that the consistency of our previous assumptions. The energy of the ideal gas is known to be

$$E = N\, \frac{d k_{\mathrm{B}} T}{2} = N\, \bar{\epsilon} \tag{83}$$

with the mean kinetic energy of each particle $\bar{\epsilon} = d k_{\mathrm{B}} T/2$. As a consequence of both the Sackur-Tetrode formula (82) for entropy and the energy equation of state (83) we obtain Gibbs' relation [29]

$$dE = T\, dS - P\, dV + \mu\, dN \tag{84}$$

with the pressure equation of state

$$P\, V = N\, k_{\mathrm{B}}\, T \tag{85}$$

and the chemical potential

$$\mu = k_{\mathrm{B}}\, T\, \ln \frac{N (2\pi\hbar)^d}{V (2\pi m k_{\mathrm{B}} T)^{\frac{d}{2}}} \tag{86}$$

If we define the local densities of energy and entropy respectively as

$$e = \frac{E}{V} \qquad \text{and} \qquad s = \frac{S}{V} \tag{87}$$

we obtain the local Gibbs' relation

$$de = T\, ds + \mu\, dn \tag{88}$$

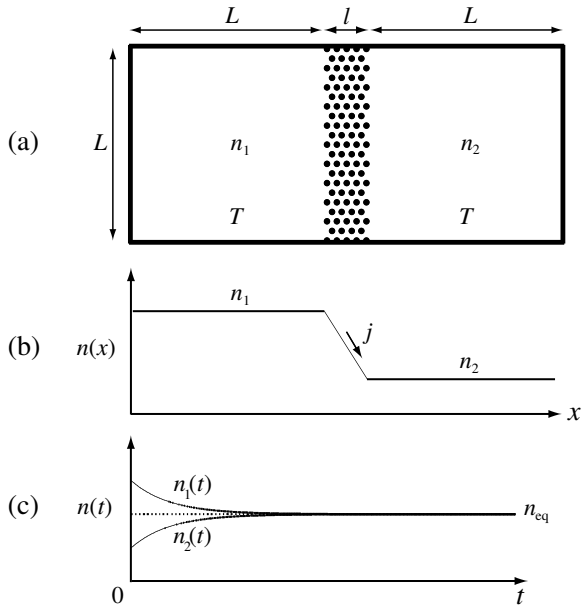

FIG. 13: Irreversible process of diffusion across a Lorentz slab leading to the equilibration of densities between both reservoirs: (a) configuration of the system; (b) initial density profile across the system; (c) time evolution of the densities which decay to their equilibrium value in each reservoir.

of local thermodynamic equilibrium at the basis of irreversible thermodynamics [29]. It is then a consequence of the diffusion equation (73) that the local density of entropy obeys the equation

$$\partial_t\, s = -\vec{\nabla}\cdot\vec{J}_s + \sigma_s \tag{89}$$

with an entropy current $\vec{J}_s$ and the local entropy production

$$\sigma_s = \bar{\mathcal{D}}\,\frac{(\vec{\nabla}n)^2}{n} \geq 0 \tag{90}$$

which is always nonnegative by the second law of thermodynamics. The calculation can be carried out *ab initio* at the microscopic level of description starting from the hydrodynamic modes of diffusion which has been discussed in the previous sections, as shown elsewhere [74, 85–88]. The detailed calculation shows that the positivity of the entropy production comes from the singular character of the hydrodynamic modes of diffusion and of the nonequilibrium steady state. This result is very natural because the singular character of the nonequilibrium states has its origin in the mixing property of the dynamics at the microscopic level as aforementioned. Our result therefore appears as the development of the intuitive idea that the positivity of the entropy production has its origin in the mixing induced in phase space, in particular, by the stretching and folding mechanism of a chaotic dynamics.

The entropy production (90) is physical as the following reasoning shows. Let us consider a slab of the Lorentz gas of width l between two large cubic reservoirs of the same volume $V = L^d$ containing respectively N_1 and N_2 light particles so that the particle densities in the reservoirs are respectively $n_1 = N_1/V$ and $n_2 = N_2/V$ (see Fig. 13). The velocity distribution can be taken to be a Maxwell-Boltzmann distribution at the same temperature T across the whole system. Since the diffusion process is isothermal the temperature T remains constant through the whole process and there is no heat produced. However, there is a current of particles equal to $j = \bar{\mathcal{D}}(n_1 - n_2)/l$ from the high-density reservoir to the low-density one because of the difference of concentrations across the Lorentz slab. This is an example of a process of exchange of matter as they are encountered in chemical thermodynamics. In such processes, a current is possible without simultaneous heat production. The current of particles decreases the difference of densities between both reservoirs. As long as there is a difference of densities the system is out of equilibrium until the thermodynamic equilibrium is reached when $n_1(t=\infty) = n_2(t=\infty) = n_{\rm eq} = (N_1+N_2)/(2V)$ so that the current vanishes. The irreversible process of equilibration by the diffusion of particles across the Lorentz slab leads to a production of entropy. Indeed, in the initial situation, the entropy of the whole system is equal to the entropies of both reservoirs if the Lorentz slab is supposed to be smaller than the reservoirs ($l \ll L$) so that its

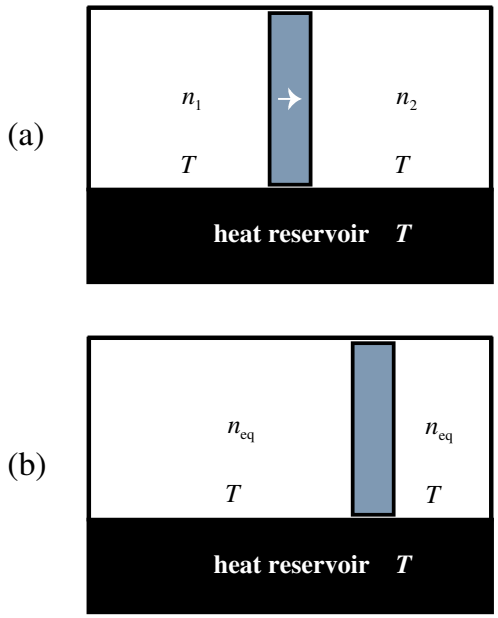

FIG. 14: Replacement of the Lorentz slab by a movable piston so that work can be extracted from the difference of densities if the whole system is in contact with a heat reservoir: (a) initial configuration of the system; (b) final configuration after the work W has been extracted.

entropy is negligible:

$$S_{\rm initial} = S_1 + S_2 \qquad \text{with} \quad S_1 = k_{\rm B} N_1 \ln \frac{cV}{N_1} \quad \text{and} \quad S_2 = k_{\rm B} N_2 \ln \frac{cV}{N_2} \tag{91}$$

with a constant c depending on temperature. The entropy after equilibration is given by

$$S_{\rm final} = k_{\rm B}(N_1 + N_2) \ln \frac{c\, 2V}{N_1 + N_2} \tag{92}$$

so that the total entropy production is

$$\Delta S = S_{\rm final} - S_{\rm initial} = k_{\rm B} N_1 \ln \frac{2N_1}{N_1 + N_2} + k_{\rm B} N_2 \ln \frac{2N_2}{N_1 + N_2} \tag{93}$$

$$\geq k_{\rm B} N_1 \left(1 - \frac{N_1 + N_2}{2N_1} \right) + k_{\rm B} N_2 \left(1 - \frac{N_1 + N_2}{2N_2} \right) = 0 \tag{94}$$

because of the inequality $\ln(1/x) \geq 1 - x$. Accordingly, the entropy production (94) which can be rewritten in the form

$$\Delta S = k_{\rm B} N_1 \ln \frac{n_1}{n_{\rm eq}} + k_{\rm B} N_2 \ln \frac{n_2}{n_{\rm eq}} \tag{95}$$

is positive in the above isothermal process. The process is thus irreversible in the sense of the second law of thermodynamics.

Moreover, the entropy production (95) corresponds to some work which could otherwise be used if we replaced the Lorentz slab by a movable piston of equal volume and if the system was put in contact with a heat reservoir (see Fig. 14). In the initial situation where there is a difference of particle densities between both sides, the piston is submitted to a force due to the difference of pressures

$$P_{1,\rm initial} = \frac{N_1 k_{\rm B} T}{V} \qquad \text{and} \qquad P_{2,\rm initial} = \frac{N_2 k_{\rm B} T}{V} \tag{96}$$

This force can produce a work if the piston is slowly moved until both pressures equilibrate. We suppose that the piston is moved so slowly that the process be isothermal. The equilibrium of pressures is reached when the high-density, high-pressure fluid has expanded and compressed the fluid on the other side so that both have the same

equilibrium density $n_{\rm eq}$, the temperature T being kept constant. The volumes of both fluids have changed so that

$$n_{\rm eq} = \frac{N_1}{V_1} = \frac{N_2}{V_2} = \frac{N_1+N_2}{2V} \qquad \text{and} \qquad P_{1,\rm final} = \frac{N_1 k_{\rm B} T}{V_1} = P_{2,\rm final} = \frac{N_2 k_{\rm B} T}{V_2} \tag{97}$$

with $V_1 + V_2 = 2V$, the numbers of particles being here constant in each fluids. The work extracted in this process is

$$W = \int_{\rm initial}^{\rm final} P_1 \, dV_1 + P_2 \, dV_2 = k_{\rm B} T \left(N_1 \ln \frac{V_1}{V} + N_2 \ln \frac{V_2}{V} \right) \tag{98}$$

Since the ratios of volumes are equal to the ratios of densities

$$\frac{V_1}{V} = \frac{n_1}{n_{\rm eq}} \qquad \text{and} \qquad \frac{V_2}{V} = \frac{n_2}{n_{\rm eq}} \tag{99}$$

we find that the extracted work is equal to the temperature multiplied by the entropy production of the previous process:

$$W = k_{\rm B} T \left(N_1 \ln \frac{n_1}{n_{\rm eq}} + N_2 \ln \frac{n_2}{n_{\rm eq}} \right) = T \, \Delta S \tag{100}$$

Since the initial and final energies of the particles in both fluids are equal by the equation of state (83), the work W has been pumped from the heat reservoir. Accordingly, we conclude that the entropy (95) produced by diffusion corresponds to some work which is lost in the process of diffusion. In this sense, the diffusion process dissipates an energy which could otherwise be used, which confirms that diffusion in the Lorentz gas is an irreversible process obeying the second law of thermodynamics.

V. DECAY AND RELAXATION IN QUANTUM SYSTEMS

Recent work has shown that different regimes exist in the relaxation of a quantum system [21–28]. One regime is the famous golden rule regime in the case of weak coupling. This relaxation proceeds slowly between the energy levels of a noninteracting system because of the weak coupling between these levels due to a perturbing interaction.

Another regime is the semiclassical regime in classically chaotic systems. In the semiclassical limit, the time correlation functions of the quantum dynamics have an early decay which follows the classical dynamics and its Pollicott-Ruelle resonances. Therefore, the decay rate of the quantum time correlation function becomes equal to the decay rate of the leading Pollicott-Ruelle resonance. In simple systems such as the dyadic baker map or the standard map at large values of the parameter K the leading nontrivial Pollicott-Ruelle resonance is essentially given by the positive Lyapunov exponent. For this reason, this regime is sometimes referred to as the "Lyapunov regime" [27, 28].

In the following, we shall focus on the semiclassical regime and explain how the Pollicott-Ruelle resonances emerge from the quantum dynamics.

Let us consider a quantum time correlation function of an observable $\hat{A}$ defined with respect to an equilibrium density matrix $\hat{\rho} = p(\hat{H})$ where $\hat{H}$ is the Hamiltonian operator of the system:

$$\langle \hat{A}(t) \hat{B}(0) \rangle \equiv \mathrm{tr} \; p(\hat{H}) \; \hat{A}(t) \; \hat{B}(0) \tag{101}$$

The time evolution is determined by the Hamiltonian according to the Schrödinger equation as

$$\hat{X}(t) = \exp(+\mathrm{i}\hat{H}t/\hbar) \; \hat{X} \; \exp(-\mathrm{i}\hat{H}t/\hbar) \tag{102}$$

The correlation function (101) is related to the one defined on the microcanonical ensemble

$$C_E(t) \equiv \mathrm{tr} \; \delta(E - \hat{H}) \; \hat{A}(t) \; \hat{B}(0) \tag{103}$$

by

$$\langle \hat{A}(t) \hat{B}(0) \rangle = \int dE \; p(E) \; C_E(t) \tag{104}$$

If the system is closed the energy spectrum is discrete and the time evolution can be decomposed on the energy eigenstates

$$\hat{H} |n\rangle = E_n |n\rangle \tag{105}$$

so that the time correlation function becomes

$$\langle \hat{A}(t)\hat{B}(0)\rangle = \sum_{m,n} p(E_m)\ A_{mn}\ B_{nm}\ \mathrm{e}^{+\frac{\mathrm{i}}{\hbar}(E_m-E_n)\ t} \tag{106}$$

This is an almost-periodic function of time presenting an early decay followed by quantum fluctuations due to the discreteness of the energy spectrum. The quantum fluctuations manifest themselves on time scales longer than the Heisenberg time which is the time of resolution of the energy levels by using a time Fourier transform. For shorter times, the individual energy levels cannot be resolved and the time correlation function decays as if the spectrum was continuous. Since the level density is huge in many-body systems the Heisenberg time is more than cosmological and the energy spectrum can be assumed to be quasi-continuous.

At room temperature, the de Broglie wavelength is smaller than the mean free path and the semiclassical approximation is most appropriate in order to evaluate the time correlation function [89–92]. This is performed by first using the Weyl-Wigner expansion in which the operators $\hat{X}$ are transformed into functions $X_{\rm cl}(\{\vec{r}_i,\vec{p}_i\}_{i=1}^N)$ defined on the phase space of positions and momenta. Quantum oscillations are then taken into account by Gutzwiller's periodic-orbit corrections [93]. The semiclassical expansion can be carried out on the correlation function (103) defined for the microcanonical ensemble to get [91, 92]

$$\begin{aligned} C_E(t) &= \int \frac{d^f r d^f p}{(2\pi\hbar)^f}\ \delta(E-H_{\rm cl})\ A_{\rm cl}(t)\ B_{\rm cl}(0) + O(\hbar^{-f+1}) \\ &+ \frac{1}{\pi\hbar}\sum_p \sum_{r=1}^{\infty} \frac{\cos\left[\frac{r}{\hbar}S_p(E) - r\frac{\pi}{2}\mu_p\right]}{|\det(\mathbf{I}-\mathbf{m}_p^r)|^{\frac{1}{2}}} \oint_p A_{\rm cl}(\tau+t)B_{\rm cl}(\tau)d\tau + O(\hbar^0) \end{aligned} \tag{107}$$

where the classical observables evolve according to

$$X_{\rm cl}(t) = \exp(-\hat{\mathcal{L}}_{\rm cl}t)\ X_{\rm cl}(0) \tag{108}$$

with the classical Liouvillian operator $\hat{\mathcal{L}}_{\rm cl} \equiv \{H_{\rm cl},\cdot\}$. The leading term in Eq. (107) is precisely the classical correlation function which decays under the effect of the Frobenius-Perron operator and of its Pollicott-Ruelle resonances [22, 23, 91, 92]. Beside the leading term, there is a Weyl-Wigner series of quantum corrections in powers of the Planck constant which can be computed by a similar method as the leading term. Beyond the Weyl-Wigner series, there are the periodic-orbit corrections given by a sum over all the unstable periodic orbits and their repetitions $r = 1, 2, 3, ...$, the system being assumed to be hyperbolic. The correction of the periodic orbit p depends on its reduced action $S_p(E) = \sum_{i=1}^N \oint_p \vec{p}_i \cdot d\vec{r}_i$, its Maslov index μ_p, its linearized Poincaré map $\mathbf{m}_p$, as well as the time correlation function calculated over the periodic orbit p. When the number of degrees of freedom $f = Nd$ increases the periodic-orbit corrections become negligible with respect to the leading terms of the Weyl-Wigner series.

A similar expansion holds for the quantum survival probability in open quantum systems such as the disk scatterers [20] and the open quantum graphs [24]. The survival probability of a particle in a domain $\mathcal{S}$ of indicator function $\chi(\vec{r})$ is defined by

$$P(t) \equiv \int_{\mathcal{S}} |\psi_t(\vec{r})|^2\ d\vec{r} = \mathrm{tr}\ \hat{\chi(\vec{r})}\ \mathrm{e}^{-\frac{\mathrm{i}}{\hbar}\hat{H}t}\ \hat{\rho}_0\ \mathrm{e}^{+\frac{\mathrm{i}}{\hbar}\hat{H}t} \tag{109}$$

with the initial density matrix $\hat{\rho}_0 = |\psi_0\rangle\langle\psi_0|$. The survival probability can be written in the form of a time correlation function as

$$P(t) = \int dE\ \mathrm{tr}\ \delta(E-\hat{H})\ \hat{\rho}_0\ \mathrm{e}^{+\frac{\mathrm{i}}{\hbar}\hat{H}t}\ \hat{\chi(\vec{r})}\ \mathrm{e}^{-\frac{\mathrm{i}}{\hbar}\hat{H}t} \tag{110}$$

In the semiclassical limit, the survival probability becomes

$$\begin{aligned} P(t) &= \int \frac{d^f r\ d^f p}{(2\pi\hbar)^f}\ \rho_{0\rm cl}\ \mathrm{e}^{-\hat{\mathcal{L}}_{\rm cl}t}\chi_{\rm cl} + O(\hbar^{-f+1}) \\ &+ \frac{1}{\pi\hbar}\int dE \sum_p \sum_{r=1}^{\infty} \frac{\cos\left[\frac{r}{\hbar}S_p(E) - r\frac{\pi}{2}\mu_p\right]}{|\det(\mathbf{I}-\mathbf{m}_p^r)|^{1/2}} \oint_p \rho_{0\rm cl}\ \mathrm{e}^{-\hat{\mathcal{L}}_{\rm cl}t}\chi_{\rm cl}\ d\tau + O(\hbar^0) \end{aligned} \tag{111}$$

Here also, the time evolution of the leading term is ruled by the classical Frobenius-Perron operator so that the early decay of the survival probability is determined by the Pollicott-Ruelle resonances [20–24].

This result applies in particular to the scattering of waves on disk scatterers [14, 20]. These systems have been studied in remarkable microwave experiments by Sridhar and coworkers, who have been able to obtain not only the escape rate but also the next Pollicott-Ruelle resonances of the two-, three- and four-disk scatterers [21].

We can thus say that the classical decay and its Pollicott-Ruelle resonances emerge out of the wave-mechanical dynamics. The Pollicott-Ruelle resonances are therefore important to understand the relaxation of a system not only in the classical context but also in the quantum one.

In simple systems such the K-adic baker maps defined as

$$(x_{n+1}, y_{n+1}) = \left(K x_n - l, \frac{y_n + l}{K} \right) \qquad \text{for} \quad \frac{l}{K} < x_n < \frac{l+1}{K} \qquad (l = 0, 1, 2, ..., K-1) \tag{112}$$

the Pollicott-Ruelle resonances are integer multiples of the positive Lyapunov exponent $\lambda = \ln K$: $s_j = -j\lambda$ with $j = 0, 1, 2, 3, ...$ The reason is that the dynamics acts by a uniform stretching in the K-adic baker maps. The leading nontrivial Pollicott-Ruelle resonance of the standard map is also well approximated by the Lyapunov exponent at large values of the parameter K: $s_1 \approx -\lambda$. However, for general baker maps without a uniform stretching, the Pollicott-Ruelle resonances differ from multiples of the Lyapunov exponent [25]. Therefore, the connection between the decay rates and the Lyapunov exponent is not general. Instead, the decay rates are directly given by the Pollicott-Ruelle resonances which may become very small in spatially extended systems where they can connect to the hydrodynamics, although the Lyapunov exponents keep a value corresponding to the time scale of kinetics.

VI. CONCLUSIONS

Thanks to the recent advances in dynamical systems theory, we have a better understanding of the dynamical basis of the macroscopic behavior of matter and, especially, of the mechanisms of relaxation toward the thermodynamic equilibrium. This understanding also concerns the nonequilibrium steady states.

An important role is played by Gibbs' property of mixing in the phase space of the underlying microscopic system. Dynamical chaos characterized by positive Lyapunov exponents and KS entropy induces the stretching and folding of phase-space volumes and provides an effective mechanism of mixing. This chaotic mixing generates fractal structures at the phase-space level of description when an explicit construction is carried out of the nonequilibrium objects or states such as the fractal repeller selected by absorbing boundary conditions, the hydrodynamic modes selected by quasiperiodic boundary conditions, or the nonequilibrium steady states selected by flux boundary conditions.

Different nonequilibrium states are thus selected by different boundary conditions which mathematically express the way nonequilibrium constraints are imposed on the system. As explained in Subsection III B, the nonequilibrium constraint can be imposed within the Liouvillian formulation of statistical mechanics in agreement with a Hamiltonian volume-preserving microscopic dynamics obeying Liouville's theorem of classical mechanics. In this way, Liouvillian thermostats are defined which can describe at the microscopic statistical level a broad variety of nonequilibrium systems from linearly conducting regimes close to the thermodynamic equilibrium to far-from-equilibrium regimes sustaining the Rayleigh-Bénard convection or other macroscopic fluid instabilities, as well as nonlinear chemical instabilities [94].

The Liouvillian statistical formulation leads, in particular, to the construction of the hydrodynamic and reactive modes which rule the long-time relaxation toward the thermodynamic equilibrium. The dispersion relations of the hydrodynamic modes can be given in terms of the Pollicott-Ruelle resoances. The modes themselves are the eigenstates associated with the Pollicott-Ruelle resonances and they can be constructed by a kind of renormalization semigroup generated by the time evolution of statistical ensembles of trajectories from the initial time to infinity [42]. The point-like nature of classical mechanics and the mixing property only allow a weak convergence to a statistical state of thermodynamic equilibrium. Thanks to the renormalization semigroup, modes of pure exponential decay can be constructed in hyperbolic systems with positive Lyapunov exponents.[109] These modes are represented by a singular density which is not a regular function as is the case in stochastic processes but a mathematical distribution or generalized function in the sense of Schwartz and Gel'fand [95, 96]. If the underlying dynamics is chaotic (i.e., has a positive KS entropy), the cumulative function of these modes are fractal. In this context, relationships can be established between the irreversible properties and the characteristic quantities of chaos. These relationships have been obtained, in particular, for diffusion and reaction-diffusion in the Lorentz gases as well as in the multibaker models. These processes of exchange of matter obey the second law of thermodynamics consistently at the macroscopic level as explained in Subsection IV F and at the microscopic level because of the singular character of the nonequilibrium states [74, 85–88].

At the quantum-mechanical level of description, the emergence of classical relaxation can be understood thanks to the semiclassical method and Gutwiller's trace formula. The quantum time correlation functions can be expressed by a Weyl-Wigner series corrected by periodic-orbit contributions. The leading term of the Weyl-Wigner series is the

classical time correlation function which decays according to the Pollicott-Ruelle resonances as explained in Section V. In simple models, the Pollicott-Ruelle resonances correspond to the "Lyapunov decay regime" which have been recently investigated beside the "golden rule decay regime" [26–28]. All these results show that various processes of decay and relaxation can effectively be understood thanks to the recent advances in dynamical systems theory.

Acknowledgments. The author thanks Professor G. Nicolis for support and encouragement in this research. The author and this research are financially supported by the National Fund for Scientific Research (F. N. R. S. Belgium).

APPENDIX A: EXPONENTIAL DECAY IN THE INVERTED HARMONIC POTENTIAL

The inverted harmonic potential appears for instance in the vicinity of the maximum of the potential in the Hamiltonian system (39) [3]. If this Hamiltonian is restricted to quadratic terms and if a canonical transformation is carried out to the new canonical coordinates which are the x-coordinate along the unstable manifold and the y-coordinate along the stable manifold, we obtain the Hamiltonian

$$H = \lambda\, x\, y \tag{A1}$$

The solution of Hamilton's equations

$$\begin{cases} \dot{x} = +\frac{\partial H}{\partial y} = +\lambda\, x \\ \dot{y} = -\frac{\partial H}{\partial x} = -\lambda\, y \end{cases} \tag{A2}$$

is the flow

$$\Phi^t(x,y) = \left(\mathrm{e}^{+\lambda t}x, \mathrm{e}^{-\lambda t}y\right) \tag{A3}$$

In the long-time limit $t \to +\infty$, $\exp(-\lambda t)$ is a small parameter in terms of which we can carried out a Taylor expansion of the statistical averages according to [3]

$$\langle A\rangle_t = \int dx\, dy\, f_0(x,y)\, A\Big(\underbrace{\mathrm{e}^{+\lambda t}x}_{=x'}, \mathrm{e}^{-\lambda t}y\Big) \tag{A4}$$

$$= \mathrm{e}^{-\lambda t} \int dx'\, dy\, f_0\left(\mathrm{e}^{-\lambda t}x', y\right)\, A\left(x', \mathrm{e}^{-\lambda t}y\right) \tag{A5}$$

$$= \mathrm{e}^{-\lambda t} \int dx'\, dy \sum_{l=0}^{\infty} \frac{1}{l!}\, \mathrm{e}^{-\lambda l t}\, x'^l\, \partial_x^l f_0(0,y) \sum_{m=0}^{\infty} \frac{1}{m!}\, \mathrm{e}^{-\lambda m t}\, y^m\, \partial_y^m A(x',0) \tag{A6}$$

$$= \sum_{l,m=0}^{\infty} \mathrm{e}^{-\lambda(l+m+1)t}\, \frac{1}{m!} \int dx'\, x'^l\, \partial_y^m A(x',0)\, \frac{1}{l!} \int dy\, y^m\, \partial_x^l f_0(0,y) \tag{A7}$$

$$= \sum_{l,m=0}^{\infty} \mathrm{e}^{-\lambda(l+m+1)t}\, \langle A|\Psi_{lm}\rangle\, \langle\tilde{\Psi}_{lm}|f_0\rangle \tag{A8}$$

where the eigenstates can be identified as

$$\Psi_{lm}(x,y) = \frac{1}{m!}\, x^l\, (-\partial_y)^m\, \delta(y) \tag{A9}$$

$$\tilde{\Psi}_{lm}(x,y) = \frac{1}{l!}\, y^m\, (-\partial_x)^l\, \delta(x) \tag{A10}$$

The eigenstates are given by the derivatives of the Dirac distribution. The right-eigenstates Ψ_{lm} have the unstable manifold $y = 0$ for support, while the left-eigenstates $\tilde{\Psi}_{lm}$ have the stable manifold $x = 0$ for support. We can check that these distributions are respectively the eigensolutions of the Liouvillian operator and of its adjoint:

$$\hat{L}\, \Psi_{lm} = -\lambda\, (l+m+1)\, \Psi_{lm} \tag{A11}$$

$$\hat{L}\, \tilde{\Psi}_{lm} = -\lambda\, (l+m+1)\, \tilde{\Psi}_{lm} \tag{A12}$$

Accordingly, the Pollicott-Ruelle resonances of the inverted harmonic potential are simply given by the integer multiples of the Lyapunov exponent λ:

$$s_{lm} = -\lambda\, (l+m+1) \tag{A13}$$

with $l, m = 0, 1, 2, 3, ...$

APPENDIX B: EXPONENTIAL RELAXATION IN THE BAKER MAP

The baker map is defined as the following area-preserving map of the unit square onto itself [52]

$$\phi(x,y) \;=\; \begin{cases} \left(2x, \frac{y}{2}\right) , & 0 \le x \le \frac{1}{2} \\ \left(2x-1, \frac{y+1}{2}\right) , & \frac{1}{2} < x \le 1 \end{cases} \tag{B1}$$

The unstable manifold are parallel to the x-axis, and the stable manifolds to the y-axis. The baker map is dynamically unstable with the positive Lyapunov exponent $\lambda = \ln 2$. Since the system is closed its KS entropy is equal to the positive Lyapunov exponent $h_{\rm KS} = \ln 2$ so that the baker map is chaotic. This map is known to be mixing with respect to the Lebesgue invariant measure on the unit square. Periodic-orbit theory shows that the Pollicott-Ruelle resonances of the baker map are

$$s_j = -\, j\, \ln 2 \qquad \text{with} \quad j = 0, 1, 2, 3, ... \tag{B2}$$

of multiplicity $m_j = j + 1$. The spectral decomposition involves Jordan blocks for the multiple resonances.

The Jordan blocks do not arise in the case where the initial probability density f_0, as well as the observable A, do not depend on the x-coordinate. We therefore assume for simplicity that

$$f_0(x,y) \;=\; \begin{cases} 1 , & 0 \le y < \frac{1}{2} \\ 0 , & \frac{1}{2} \le y \le 1 \end{cases} \tag{B3}$$

and $A(x,y) = A(y)$. In this case, as a consequence of the Euler–Maclaurin expansion [97], we find that [3]

$$\langle A \rangle_t \;=\; \langle A | \hat{P}^t | f_0 \rangle \;=\; \frac{1}{2} \int_0^1 A(y)\, dy \;+\; \sum_{j=1}^{\infty} \frac{A^{(j-1)}(1) - A^{(j-1)}(0)}{2^{jt}\; j!} \int_0^{1/2} B_j(y)\, dy \tag{B4}$$

$$\;=\; \frac{1}{2} \int_0^1 A(y)\, dy \;-\; \frac{A(1) - A(0)}{2^{t+3}} \;+\; O(2^{-3t}) \tag{B5}$$

where $A^{(j)}(y) = d^j A / dy^j$ and $B_j(y)$ is the $j^{\rm th}$ Bernoulli polynomial [97]. The first term of the asymptotic expansion of the statistical average is nothing but the long-time limit expected by the mixing property. The next term gives the slowest exponential decay. We notice that the coefficients of the exponential decays involve the values and the derivatives of the observable $A(y)$ at the ends of the unit interval where the baker map is defined, which is an unconventional feature of these expansions related to the fact that the eigenstates are mathematical distributions instead of regular functions.

APPENDIX C: HYDRODYNAMIC MODES OF DIFFUSION IN THE MULTIBAKER MAP

The multibaker map is a model of diffusion constructed by simplifying the Birkhoff map of the Lorentz gas. Different multibaker models have been constructed corresponding to different Lorentz models (see Fig. 15) [3, 71, 77, 86, 87, 98–101]. A dyadic area-preserving version of the multibaker map is defined by the following mapping which acts on a chain of unit squares [77]

$$\phi(\ell,x,y) \;=\; \begin{cases} \left(\ell - 1, 2x, \frac{y}{2}\right) , & 0 \le x \le \frac{1}{2} \\ \left(\ell + 1, 2x-1, \frac{y+1}{2}\right) , & \frac{1}{2} < x \le 1 \end{cases} \tag{C1}$$

where $\ell \in \mathbb{Z}$ denotes the label of a square which is stretched, cut in two pieces, and mapped on the next-neighboring squares $\ell \pm 1$. This phase-space dynamics induces jumps of the particle along the chain of squares. These jumps generate a symmetric random walk with diffusion coefficient $\mathcal{D} = 1/2$. The dynamics of the multibaker is time-reversal symmetric under the involution $I(\ell,x,y) = (\ell, 1-y, 1-x)$ so that $\phi^{-1} = I \circ \phi \circ I$. The dyadic multibaker (C1) is hyperbolic with the positive Lyapunov exponent $\lambda = \ln 2$ and chaotic with the KS entropy $h_{\rm KS} = \lambda = \ln 2$. Moreover, the multibaker is mixing as the hard-disk Lorentz gas.

The time evolution of statistical ensembles of noninteracting particles moving in the multibaker chain can be studied by spatial Fourier transform of the Frobenius-Perron operator. The resulting Pollicott-Ruelle resonances are given by

$$s_{j,k} = -j\, \ln 2 + \ln \cos k \tag{C2}$$

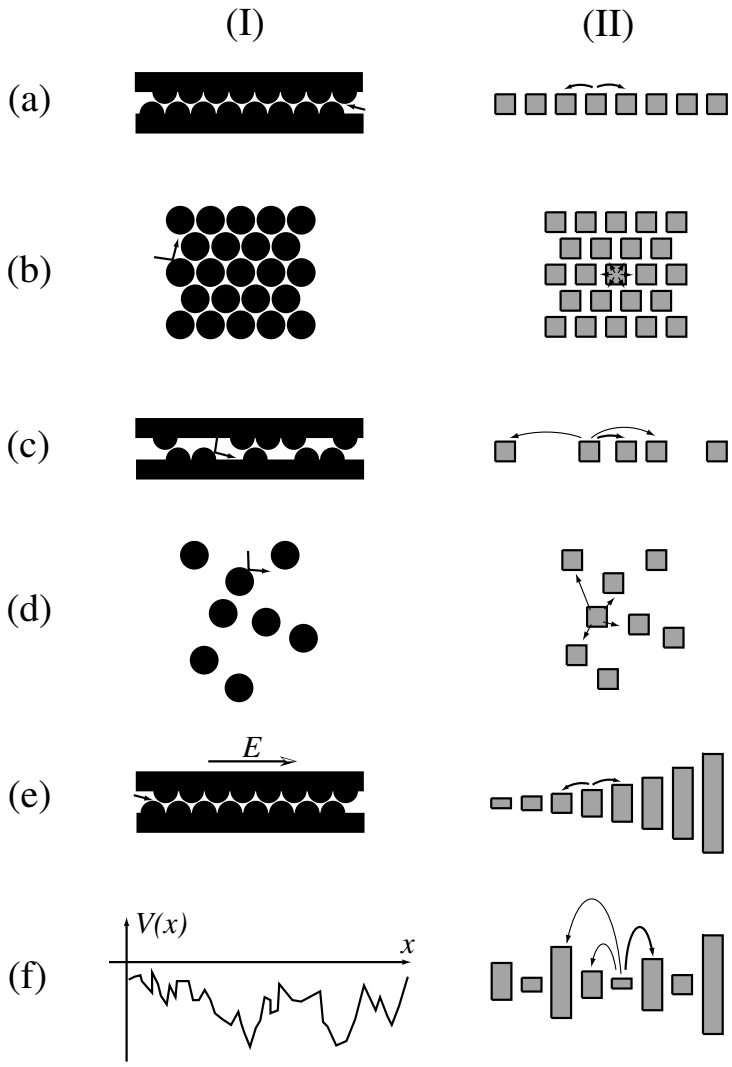

FIG. 15: Schematic representation of different Lorentz gases (I) and their corresponding multibaker model (II) for configurations of scatterers which are: (a) one-dimensional and periodic; (b) two-dimensional and periodic; (c) one-dimensional and disordered; (d) two-dimensional and disordered; (e) with a constant electric field E; (f) with a disordered potential $V(x)$.

where $k \in (-\pi, +\pi)$ is the wavenumber and $j = 0, 1, 2, 3, ...$ The hydrodynamic modes correspond to the leading Pollicott-Ruelle resonance with $j = 0$ so that the dispersion relation of these modes is given by

$$s_{0,k} = \ln \cos k = -\frac{1}{2}\, k^2 - \frac{1}{12}\, k^4 + \cdots \tag{C3}$$

which allows us to identify the diffusion coefficient $\mathcal{D} = 1/2$ as well as the super-Burnett coefficient $\mathcal{B} = -1/12$. For small nonvanishing wavenumber k, the associated eigenstates have a singular density but a continuous cumulative function given by a de Rham iterative equation [3, 102–104]. The cumulative functions form fractal curves in the complex plane (see Fig. 16) for the same reason as in the hard-disk and the Yukawa-potential Lorentz gases.

[1] J.-P. Eckmann and D. Ruelle, *Rev. Mod. Phys.* **57**, 617 (1985).
[2] J. R. Dorfman, *An Introduction to Chaos in Nonequilibrium Statistical Mechanics* (Cambridge University Press, Cambridge UK, 1999).
[3] P. Gaspard, *Chaos, Scattering and Statistical Mechanics* (Cambridge University Press, Cambridge UK, 1998).

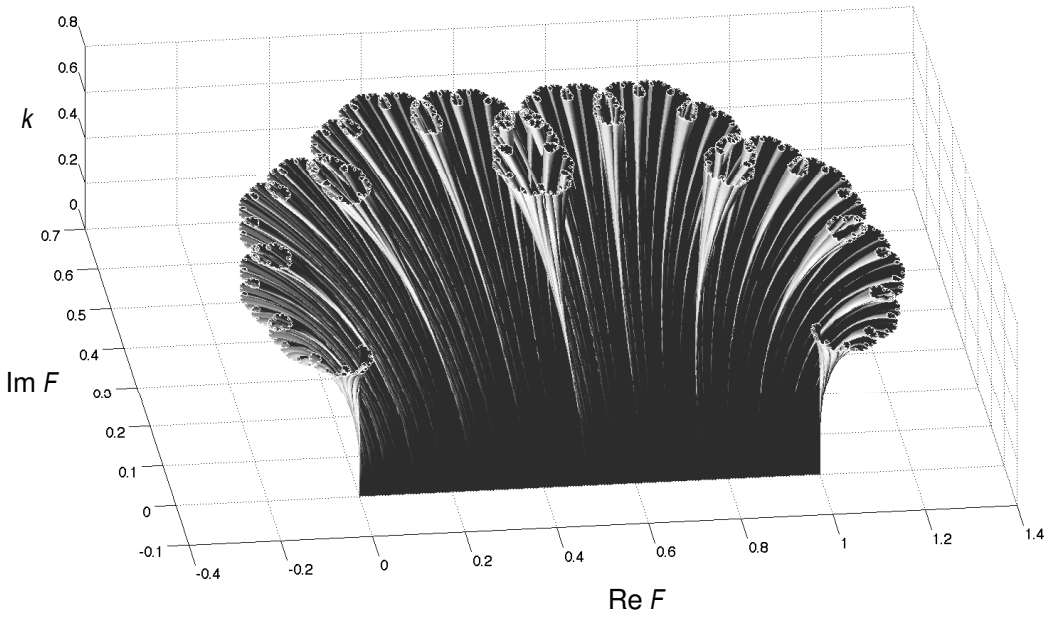

FIG. 16: Cumulative function of the hydrodynamic modes of diffusion of the dyadic multibaker map (C1). The cumulative functions $F_k(y)$ are depicted in the complex plane (Re F_k, Im F_k) versus their wavenumber k varying in the interval $0 \leq k < 0.7$. The thermodynamic equilibrium corresponds to the vanishing wavenumber $k = 0$ for which the cumulative function is $F_0(y) = y$ with $0 \leq y \leq 1$.

[4] P. Gaspard and X.-J. Wang, *Phys. Rep.* **235**, 291 (1993).
[5] I. P. Cornfeld, S. V. Fomin, and Ya. G. Sinai, *Ergodic Theory* (Springer, Berlin, 1982).
[6] M. S. Green, *J. Chem. Phys.* **20**, 1281 (1952); **22**, 398 (1954).
[7] R. Kubo, *J. Phys. Soc. Jpn.* **12**, 570 (1957).
[8] M. Pollicott, *Invent. Math.* **81**, 413 (1985).
[9] M. Pollicott, *Invent. Math.* **85**, 147 (1986).
[10] D. Ruelle, *Phys. Rev. Lett.* **56**, 405 (1986).
[11] D. Ruelle, *J. Stat. Phys.* **44**, 281 (1986).
[12] D. Ruelle, *J. Diff. Geom.* **25**, 99, 117 (1987).
[13] D. Ruelle, *Commun. Math. Phys.* **125**, 239 (1989).
[14] P. Gaspard and D. Alonso Ramirez, *Phys. Rev. A* **45**, 8383 (1992).
[15] M. Khodas and S. Fishman, *Phys. Rev. Lett.* **84**, 2837 (2000).
[16] J. Weber, F. Haake, and P. Seba, *Phys. Rev. Lett.* **85**, 3620 (2000).
[17] P. Gaspard and G. Nicolis, *Phys. Rev. Lett.* **65**, 1693 (1990).
[18] J. R. Dorfman and P. Gaspard, *Phys. Rev. E* **51**, 28 (1995).
[19] P. Gaspard and J. R. Dorfman, *Phys. Rev. E* **52**, 3525 (1995).
[20] P. Gaspard and S. A. Rice, *J. Chem. Phys.* **90**, 2225, 2242, 2255 (1989).
[21] W. Lu, M. Rose, K. Pance, and S. Sridhar, *Phys. Rev. Lett.* **82**, 5233 (1999); W. Lu, L. Viola, K. Pance, M. Rose, and S. Sridhar, *Phys. Rev. E* **61**, 3652 (2000); K. Pance, W. Lu, and S. Sridhar, *Phys. Rev. Lett.* **85** (2000).
[22] F. Haake, *Quantum Signatures of Chaos* (Springer, Berlin, 2000).
[23] O. Agam, *Phys. Rev. E* **61**, 1285 (2000).
[24] F. Barra and P. Gaspard, *Phys. Rev. E* **63**, 066215 (2001); *Phys. Rev. E* **65**, 016205 (2001).
[25] A. Jordan and M. Srednicki, *The Approach to Ergodicity in the Quantum Baker's Map*, preprint `chao-dyn/0108024` (2001).
[26] R. A. Jalabert and H. M. Pastawski, *Phys. Rev. Lett.* **86**, 2490 (2001).
[27] Ph. Jacquod, P. G. Silvestrov, and C. W. J. Beenakker, *Phys. Rev. E* **64** 055203(R) (2001).
[28] Ph. Jacquod, I. Adagideli, and C. W. J. Beenakker, *Decay of the Loschmidt echo for quantum states with sub-Planck scale structures*, preprint `nlin.CD/0203052` (2002).
[29] S. de Groot and P. Mazur, *Non-equilibrium Thermodynamics* (North-Holland, Amsterdam, 1962); reprinted by (Dover Publ. Co., New York, 1984).
[30] G. Nicolis, *Introduction to Nonlinear Science* (Cambridge University Press, Cambridge UK, 1995).
[31] S. Chapman and T. G. Cowling, *The Mathematical Theory of Non-Uniform Gases*, 3rd Edition (Cambridge University Press, Cambridge UK, 1970).

[32] L. Kadanoff and P. C. Martin, *Ann. Phys. (N.Y.)* **24**, 419 (1963).
[33] M. H. Ernst and J. R. Dorfman, *Physica* **61**, 157 (1972); *J. Stat. Phys.* **12**, 311 (1975).
[34] R. Balescu, *Equilibrium and Nonequilibrium Statistical Mechanics* (Wiley, New York, 1975).
[35] J.-P. Boon and S. Yip, *Molecular Hydrodynamics* (Dover, New York, 1980).
[36] P. Résibois and M. De Leener, *Classical Kinetic Theory of Fluids* (Wiley, New York, 1977).
[37] E. G. D. Cohen, I. M. de Schepper, and M. J. Zuilhof, *Physica B* **127**, 282 (1984).
[38] J. O. Hirschfelder, C. F. Curtiss, and R. B. Bird, *Molecular Theory of Gases and Liquids* (Wiley, New York, 1954).
[39] P. Gaspard and R. Klages, *Chaos* **8**, 409 (1998).
[40] I. Claus and P. Gaspard, *J. Stat. Phys.* **101**, 161 (2000).
[41] I. Claus and P. Gaspard, *The fractality of the relaxation modes in deterministic reaction-diffusion systems*, preprint `cond-mat/0204264` to appear in *Physica D* (2002).
[42] P. Gaspard and I. Claus, *Phil. Trans. Roy. Soc. London A* **360** (2002).
[43] K. J. Laidler, *Theories of Chemical Reaction Rates* (McGraw-Hill, New York, 1969).
[44] A. H. Zewail, *Femtochemistry: Ultrafast Dynamics of the Chemical Bond*, Vols. I-II (World Scientific, Singapore, 1994).
[45] D. Forster, *Hydrodynamic Fluctuations, Broken Symmetry, and Correlation Functions* (Benjamin/Cummings, Reading, 1975).
[46] P. D. Fleming and C. Cohen, *Phys. Rev. B* **13**, 500 (1975).
[47] P. C. Hohenberg and P. C. Martin, *Ann. Phys. (N.Y.)* **34**, 291 (1965).
[48] H. Goldstein, *Classical Mechanics* (Addison-Wesley, Reading, 1950).
[49] J.-P. Eckmann, C.-A. Pillet, and L. Rey-Bellet, *J. Stat. Phys.* **95**, 305 (1999).
[50] S. Berry, S. A. Rice, and J. Ross, *Physical Chemistry* (Wiley, New York, 1980).
[51] J. W. Gibbs, *Elementary Principles in Statistical Mechanics* (Yale University Press, New Haven, 1902); reprinted by (Dover Publ. Co, New York, 1960).
[52] V. I. Arnold and A. Avez, *Ergodic Problems of Classical Mechanics* (Benjamin, New York, 1968).
[53] R. Abraham and J. E. Marsden, *Foundations of Mechanics* (Benjamin/Cummings Publ., Reading, 1978).
[54] B. V. Chirikov, *Phys. Reports* **52**, 263 (1979).
[55] A. Katok, *Commun. Math. Phys.* **111**, 151 (1987); E. Gutkin, *Physica D* **19**, 311 (1986); E. Gutkin, *J. Stat. Phys.* **83**, 7 (1996); S. Troubetzkoy, *Chaos* **8**, 242 (1998).
[56] C. P. Dettmann and E. G. D. Cohen, *J. Stat. Phys.* **101**, 775 (2000).
[57] A. K. Zvonkin and L. A. Levin, *Russian Math. Surveys* **25**, 83 (1970).
[58] P. Gaspard and X.-J. Wang, *Proc. Natl. Acad. Sci. (USA)* **85**, 4591 (1988).
[59] J. L. Lebowitz, C. Maes, and E. R. Speer, *J. Stat. Phys.* **59**, 117 (1990).
[60] J. P. Boon, D. Dab, R. Kapral, and A. Lawniczak, *Phys. Reports* **273**, 55 (1996).
[61] J.-P. Rivet and J. P. Boon, *Lattice Gas Hydrodynamics* (Cambridge University Press, Cambridge UK, 2001).
[62] P. Gaspard, *Int. J. Mod. Phys. B* **15**, 209 (2001); reprinted in: L. H. Y. Chen, J. Packer Jesudason, C. H. Lai, C. H. Oh, K. K. Phua & Eng-Chye Tan, Eds., *Challenges for the 21st Century, Proceedings of the International Conference on Fundamental Sciences: Mathematics and Theoretical Physics, Singapore, 13-17 March 2000* (World Scientific, Singapore, 2001) pp. 398-429.
[63] P. Gaspard, G. Nicolis, A. Provata, and S. Tasaki, *Phys. Rev. E* **51**, 74 (1995).
[64] P. Gaspard and S. Tasaki, *Phys. Rev. E* **64**, 056232 (2001).
[65] P. Cvitanović and B. Eckhardt, *J. Phys. A: Math. Gen.* **24**, L237 (1991).
[66] R. Artuso, E. Aurell, and P. Cvitanović, *Nonlinearity* **3**, 325, 361 (1990).
[67] E. Helfand, *Phys. Rev.* **119**, 1 (1960).
[68] P. Gaspard and F. Baras, *Phys. Rev. E* **51**, 5332 (1995).
[69] H. van Beijeren, A. Latz, and J. R. Dorfman, *Phys. Rev. E* **63**, 016312 (2000).
[70] I. Claus and P. Gaspard, *Phys. Rev. E* **63**, 036227 (2001).
[71] T. Tél, J. Vollmer, and W. Breymann, *Europhys. Lett.* **35**, 659 (1996).
[72] P. Gaspard, *Phys. Rev. E* **53**, 4379 (1996).
[73] P. Gaspard, I. Claus, T. Gilbert, and J. R. Dorfman, *Phys. Rev. Lett.* **86**, 1506 (2001).
[74] J. R. Dorfman, P. Gaspard, and T. Gilbert, *Entropy production of diffusion in spatially periodic deterministic systems*, preprint `nlin.CD/0203046` (2002).
[75] T. Gilbert, J. R. Dorfman, and P. Gaspard, *Nonlinearity* **14**, 339 (2001).
[76] P. Gaspard, *Physica A* **240**, 54 (1997).
[77] S. Tasaki, and P. Gaspard, *J. Stat. Phys.* **81**, 935 (1995).
[78] H. A. Lorentz, *Proc. Roy. Acad. Amst.* **7**, 438, 585, 684 (1905).
[79] H. van Beijeren, *Rev. Mod. Phys.* **54**, 195 (1982).
[80] C. P. Dettmann, *The Lorentz gas as a paradigm for nonequilibrium stationary states*, in: D. Szasz, Editor, *Hard Ball Systems and Lorentz Gas*, Encycl. Math. Sci. (Springer, Berlin, 2000).
[81] L. A. Bunimovich, and Ya. G. Sinai, *Commun. Math. Phys.* **78**, 247, 479 (1980).
[82] A. Knauf, *Commun. Math. Phys.* **110**, 89 (1987); *Ann. Phys. (N. Y.)* **191**, 205 (1989).
[83] D. Alonso, R. Artuso, G. Casati, and I. Guarneri, *Phys. Rev. Lett.* **82**, 1859 (1999).
[84] R. K. Pathria, *Statistical Mechanics* (Pergamon, Oxford, 1972).
[85] P. Gaspard, *J. Stat. Phys.* **88**, 1215 (1997).
[86] S. Tasaki and P. Gaspard, *Theoretical Chemistry Accounts* **102**, 385 (1999).

[87] S. Tasaki and P. Gaspard, *J. Stat. Phys.* **101**, 125 (2000).
[88] T. Gilbert, J. R. Dorfman, and P. Gaspard, *Phys. Rev. Lett.* **85**, 1606 (2000).
[89] M. Wilkinson, *J. Phys. A: Math. Gen.* **20**, 2415 (1987).
[90] K. Richter, *Europhys. Lett.* **29**, 7 (1995); B. Mehlig and K. Richter, *Phys. Rev. Lett.* **80**, 1936 (1998).
[91] P. Gaspard and S. R. Jain, *Pramana-J. of Phys.* **48**, 503 (1997).
[92] P. Gaspard, in: J. Karkheck, Editor, *Dynamics: Models and Kinetic Methods for Non-Equilibrium Many Body Systems*, NATO ASI Series (Kluwer, Dordrecht, 2000) pp. 425-456.
[93] M. C. Gutzwiller, *Chaos in Classical and Quantum Mechanics* (Springer, New York, 1990).
[94] I. Claus, *Microscopic Chaos, Fractals, and Reaction-Diffusion Processes* (Ph. D. Thesis, Université Libre de Bruxelles, Faculty of Sciences, February 2002).
[95] N. Dunford and J. T. Schwartz, *Linear operators*, Vols. I-III (Interscience-Wiley, New York, 1958, 1963, 1971).
[96] I. Gel'fand and G. Shilov, *Generalized Functions*, Vol. 2 (Academic Press, New York, 1968).
[97] M. Abramowitz and I. A. Stegun, *Handbook of Mathematical Functions* (Dover, New York, 1972).
[98] P. Gaspard, *J. Stat. Phys.* **68**, 673 (1992).
[99] G. Radons, *Festkrperprobleme/Advances in Solid State Physics* **38**, 339 (1999).
[100] T. Tél and J. Vollmer, *Entropy Balance, Multibaker Maps, and the Dynamics of the Lorentz gas*, in: D. Szász, Editor, *Hard Ball Systems and the Lorentz Gas* (Springer-Verlag, Berlin, 2000) pp. 367-418.
[101] J. Vollmer, T. Tél, and L. Mátyás, J. Stat. Phys. **101**, 79 (2000).
[102] H. H. Hasegawa and D. J. Driebe, *Phys. Rev. E* **50**, 1781 (1994).
[103] D. J. Driebe, *Fully Chaotic Maps and Broken Time Symmetry* (Kluwer, Dordrecht, 1999).
[104] S. Tasaki and P. Gaspard, *Bussei Kenkyu Research Report in Condensed-Matter Theory* **66**, 23 (1996).
[105] The mixing is the temporal analog of the clustering property which assumes the statistical independency of two spatially separated random events or variables.
[106] Here we ignore the hydrodynamic modes associated with the local conservation of angular momentum. If the particles are assumed to be spherical their instrinsic angular momentum can be neglected and the modes of angular momentum derive from those of linear momentum [31].
[107] The internal rotation and vibration of the molecules can also be included in the Hamiltonian.
[108] The Lyapunov exponent associated with the direction of the flow is always vanishing in flows without fixed point according to a general argument [3].
[109] Exponential decay does not proceed until arbitrarily along time in nonchaotic models where the decay is numerically observed to deviate from exponential beyond a finite time [56].